

1 The "Year" of Tropical Convection (May 2008 to April 2010):
2 Climate Variability and Weather Highlights
3
4

5 *Duane E. Waliser¹, Mitch Moncrieff², David Burridge³, Andreas H. Fink⁴, Dave Gochis², B.*
6 *N. Goswami², Bin Guan¹, Patrick Harr⁶, Julian Heming⁷, Huang-Hsuing Hsu⁸, Christian*
7 *Jakob⁹, Matt Janiga¹⁰, Richard Johnson¹¹, Sarah Jones¹², Peter Knippertz¹³, Jose*
8 *Marengo¹⁴, Hanh Nguyen¹⁰, Mick Pope¹⁵, Yolande Serra¹⁶, Chris Thorncroft¹⁰, Matthew*
9 *Wheeler¹⁷, Robert Wood¹⁸, Sandra Yuter¹⁹*

10
11 ¹*Jet Propulsion Laboratory, California Institute of Technology, Pasadena, CA, USA*

12 ²*National Center for Atmospheric Research, Boulder, CO, USA*

13 ³*THORPEX International Programme Office, World Meteorological Office, Geneva, Switzerland*

14 ⁴*Institute of Geophysics and Meteorology, University of Cologne, Cologne, Germany*

15 ⁵*Indian Institute of Tropical Meteorology, Pune, India*

16 ⁶*Naval Postgraduate School, Monterey, CA, USA*

17 ⁷*United Kingdom Meteorological Office, Exeter, England*

18 ⁸*National Taiwan University, Taipei, Taiwan*

19 ⁹*Monash University, Melbourne, Australia*

20 ¹⁰*State University of New York, Albany, NY, USA*

21 ¹¹*Colorado State University, Fort Collins, CO, USA*

22 ¹²*Karlsruhe Institute of Technology, Karlsruhe, Germany*

23 ¹³*University of Leeds, Leeds, England*

24 ¹⁴*Centro de Previsão de Tempo e Estudos Climáticos, Sao Paulo, Brazil*

25 ¹⁵*Bureau of Meteorology Training Centre, Melbourne, Australia*

26 ¹⁶*University of Arizona, Tucson, AZ, USA*

27 ¹⁷*Centre for Australian Weather and Climate Research, Melbourne, Australia*

28 ¹⁸*University of Washington, Seattle, USA*

29 ¹⁹*North Caroline State University, Raleigh, NC, USA*

30
31
32
33 Submitted to the
34 Bulletin of the American Meteorological Society
35 November 2010
36 Submitted with revisions
37 July 2011
38
39
40
41

42 Corresponding author: *Duane Waliser, duane.waliser@jpl.nasa.gov, Jet Propulsion Laboratory,*
43 *MS 183-505, California Institute of Technology, 4800 Oak Grove Drive, Pasadena, CA 91109*

1 **Capsule Summary**

2 May 2008 to April 2010 provided a diverse array of scientifically interesting socially
3 important weather and climate events that emphasizes the impact and reach of tropical
4 convection over the globe.

5 **Abstract**

6 The representation of tropical convection remains a serious challenge to the skillfulness
7 of our weather and climate prediction systems. To address this challenge, the World Climate
8 Research Program (WCRP) and World Weather Research Program (WWRP)/THORPEX are
9 conducting a joint research activity consisting of a focus period approach along with an
10 integrated research framework tailored to exploit the vast amounts of existing observations,
11 expanding computational resources and the development of new, high-resolution modeling
12 frameworks. The objective of the Year of Tropical Convection (YOTC) is to use these
13 constructs to advance the characterization, modeling, parameterization and prediction of
14 multi-scale tropical convection, including relevant two-way interactions between tropical and
15 extra-tropical systems. This article highlights the diverse array of scientifically interesting and
16 socially important weather and climate events associated with the WCRP-WWRP/THORPEX
17 YOTC period of interest: May 2008 to April 2010. Notable during this two-year period was the
18 change from cool to warm El Nino Southern Oscillation (ENSO) states and the associated
19 modulation of a wide range of smaller time and space scale tropical convection features. This
20 period included a near record-setting wet N. American monsoon in 2008 and a very severe
21 monsoon drought in India in 2009. There was also a plethora of tropical wave activity
22 including easterly waves, the Madden-Julian Oscillation and convectively-coupled equatorial
23 wave interactions. Numerous cases of high impact rainfall events occurred along with notable
24 features in the tropical cyclone record. The intent of this article is to highlight these features
25 and phenomena, and in turn promote their interrogation via theory, observations and models
26 in concert with the YOTC program so that improved understanding and predictions of tropical
27 convection can be afforded.

1 **1 Introduction**

2 The realistic representation of tropical convection in our global atmospheric models is a
3 long-standing grand challenge for numerical weather forecasts and global climate predictions
4 (see companion article Moncrieff et al. 2011; hereafter M11). Our lack of fundamental
5 knowledge and practical capabilities in this area leaves us disadvantaged in simulating and/or
6 predicting prominent phenomena of the tropical atmosphere such as the Intertropical
7 Convergence Zone (ITCZ), El Nino – Southern Oscillation (ENSO), monsoons and their
8 active/break periods, the Madden-Julian Oscillation (MJO), easterly waves and tropical
9 cyclones, subtropical stratus decks, and even the diurnal cycle. Furthermore, tropical climate
10 and weather disturbances strongly influence stratospheric-tropospheric exchange and the
11 extra-tropics. To address this challenge, the World Climate Research Program (WCRP) and
12 World Weather Research Program (WWRP)/THORPEX jointly proposed and are
13 implementing a coordinated research program involving observing, modeling and forecasting
14 of organized tropical convection – referred to as the “Year of Tropical Convection” (see
15 www.ucar.edu/yotc). A key component of the motivation of YOTC is that there have been
16 substantial investments in the Earth Science infrastructure over the previous decades. These
17 are now realized in terms of a comprehensive satellite observing system (e.g., Earth Observing
18 System), operational buoy arrays in each of the tropical oceans, global analyses and forecast
19 systems that are now carried out at resolutions less than 25km, and a number of global, high-
20 resolution, convection-permitting modeling systems. Based on these investments, including
21 field programs already in place, a key precept of YOTC is that a tractable and promising
22 research program can be constructed from the presently available resources, through a focus
23 period approach, in much the same way field programs and specific phenomenological cases
24 focus and magnify the community’s attention and efforts (e.g., First Global GARP Experiment
25 (FGGE), TOGA COARE).

26 The YOTC period is May 2008 to April 2010; its choice developed from deliberations that
27 started with the activity’s conception at a WCRP-THORPEX sponsored meeting in 2006
28 [Moncrieff et al. 2007], its subsequent Science Planning meeting in 2007 [Waliser and
29 Moncrieff 2008], and the YOTC Implementation Planning meeting in 2009 (see
30 Implementation Plan at www.ucar.edu/yotc). While the target period was initially designed to
31 be a year, its extension to a full two years was proposed and agreed to at the Implementation
32 Planning meeting in concert with the realization that a second year would allow YOTC to
33 capture a period of both La Nina and El Nino conditions (see Figure 1). In this article, we
34 describe this period in terms of its anomalous low-frequency characteristics as well as
35 highlight the most interesting and impactful synoptic features. The description of the latter is
36 largely aligned with the targeted phenomenological areas outlined in the YOTC Science Plan.
37 These include: 1) the MJO and other convectively-coupled equatorial waves (CCEWs), 2)
38 easterly waves and tropical cyclones (TCs), 3) monsoons, 4) tropical-extratropical
39 interactions, and 5) the diurnal cycle. The objective of this overview article is to set the stage
40 for more targeted and in depth observation, modeling and prediction studies for the YOTC
41 period, following the strategies outlined in the YOTC Implementation Plan. Following the
42 descriptions of the low-frequency and synoptic characteristics is a Summary and Discussion
43 section that highlights the more notable features of the period. It concludes with an overview
44 of YOTC’s plans to leverage these features and events for case-study research to improve our
45 understanding, modeling and prediction capabilities associated with tropical convection.

2 Background Conditions and Low-Frequency Variability

Some elements of weather and higher frequency climate variability that are targeted by YOTC depend on characteristics of the conditions set up by lower-frequency climate variability. For example, the spatial characteristics and manifestations of intraseasonal variability (e.g., MJO) can be modified by the conditions of ENSO and the Indian Ocean Dipole [e.g., Hendon et al. 1999; Kessler 2001; Waliser et al. 2001; Lau 2005; Hendon et al. 2007; Rao et al. 2007; Ajayamohan et al. 2009]. Moreover, these low-frequency tropical climate conditions influence the manifestations of extra-tropical patterns of atmospheric variability [e.g., Horel and Wallace 1982; Renwick and Wallace 1996; Kumar and Hoerling 1998; Newman and Sardeshmukh 1998; Wallace 2000; e.g., Ambaum et al. 2001; Giannini et al. 2001; Hastenrath and Greischar 2001; Ostermeier and Wallace 2003]. For these reasons, we begin by documenting the background conditions and evolution of low-frequency climate patterns, including a couple of the more significant extra-tropical modes of climate variability. Figure 1 shows the anomalous characteristics of sea surface temperature (SST) in the three tropical ocean basins during the YOTC period. Starting with the Pacific, the early half the YOTC period is characterized by modest La Nina conditions while the latter half is characterized by modest El Nino conditions. Closer examination shows that the 2008-09 boreal winter period is cool and the 2009-10 boreal winter period is warm, both spring-to-summer periods tend to exhibit warming conditions, and the 2008 (2009) boreal fall undergoes cooling (warming) conditions. Overall the largest and longer-lived anomalous conditions tend to be more strongly exhibited in the western half of the Pacific basin compared to the eastern half. This evolution in anomalous SST (i.e. La Nina vs El Nino) between the first and second half of the YOTC period represents an excellent contrast for studying its effects on tropical convection characteristics.

For the Indian Ocean, there is some similarity to the Pacific, with a tendency towards cool (warm) conditions in the first (second) half of the YOTC period, albeit with about half or less the amplitudes exhibited in the Pacific. The characteristics of the Indian Ocean SST, particularly the anomalous east-west temperature gradient across the tropical Indian Ocean, can be linked to a number of important regional climate effects. For example, extreme September-October-November rainfall in tropical East Africa has been associated with periods when the western (eastern) Indian Ocean SST is anomalously high (low) – meaning a weakening of the normal west-to-east positive SST gradient [Black et al. 2003]. Similarly, northward propagating intraseasonal variability (ISV) has been found to be stronger and more coherent when the western (eastern) Indian Ocean SST is anomalously low (high) [Rao et al. 2007; Ajayamohan et al. 2008; Ajayamohan et al. 2009]. During most of YOTC, the Indian Ocean warmed, somewhat in concert with the Pacific Ocean. The western Indian Ocean was generally about 0.5°C warmer than the eastern Indian Ocean, indicating that the normal west-to-east temperature gradient in the Indian Ocean was weaker than normal throughout most of YOTC. For the Atlantic, the most remarkable feature is the exceptional warming that develops during the winter of 2009-10, lagging 3-6 months the warming in the Pacific [Carton and Huang 1994; Enfield and Mayer 1997]. This is a peak value when considering the record back to 1982. The southern Tropical Atlantic exhibits warm conditions over nearly all the YOTC period with peak magnitudes typical when considering the most recent three decades (not shown).

Figure 2 illustrates the time evolution and spatial patterns (see caption) of three important modes of extra-tropical variability during the YOTC period. These three extra-

1 tropical modes include the Pacific North America (PNA), Arctic Oscillation (AO), and the
2 Antarctic Oscillation (AAO)¹, and have been shown to be strongly correlated to tropical
3 convection variability and influence low-frequency weather variations [Horel and Wallace
4 1981; Wallace and Gutzler 1981; Hurrell 1996; Thompson and Wallace 1998; Deser 2000;
5 Thompson and Wallace 2000; e.g., Ambaum et al. 2001; L'Heureux and Higgins 2008; Pohl et
6 al. 2010]. The AO exhibits an overall anti-correlation with tropical Pacific and northern
7 Tropical Atlantic SSTs shown in Figure 1, being in mostly a positive (negative) phase during
8 these two oceans' cool (warm) periods. The AAO exhibits a strong anti-correlation to the
9 Pacific SSTs, particularly the western Pacific, while the PNA exhibits a correlation most
10 strongly to the eastern Pacific SSTs. Also illustrated in Figure 2 is the evolution of the Quasi-
11 biennial Oscillation (QBO) during YOTC, as indicated by the 50 hPa wind index time series.
12 For the most part, the entire period of YOTC is dominated by a westerly phase of the QBO,
13 with only the very ends of the period being relatively neutral. Finally, to comprehensively
14 describe the background conditions under which the YOTC period evolved, it is worth noting
15 that CO₂ concentration averaged over the two-year period was 386.8 ppm with a linear trend
16 of about +2.0 ppm year⁻¹ ², the solar cycle was largely in the minimum phase of the 11-year
17 cycle³, and there was no significant volcanic activity that occurred in or near the tropics.

18 **3 Tropical Waves**

19 *3.1 Madden-Julian Oscillation*

20 The MJO is of considerable interest in YOTC due to the considerable influence it has on
21 other components of our weather and climate system, including monsoon onset and breaks,
22 TCs, ENSO evolution, extra-tropical variability, etc. [Madden and Julian 1971; Zhang 2005; Lau
23 and Waliser 2011]. An overview of MJO-related tropical convective variability that occurred
24 during the YOTC period is provided in Figure 3. This figure uses satellite outgoing longwave
25 radiation (OLR) data filtered for eastward-propagating wavenumbers 1-5 and periods 30-96
26 days as a proxy for the convective variability associated with the MJO [Wheeler and Kiladis
27 1999; Wheeler and Weickmann 2001]. Six cases of relatively strong MJO activity have been
28 identified during this period, labeled (a)-(f). By this measure, the three strongest cases of
29 enhanced convection (i.e. negative OLR anomalies) associated with the MJO during YOTC were
30 in April 2009 (case d), November 2009 (case e), and January 2010 (case f). These periods of
31 MJO activity also show as being the strongest, although with different relative magnitudes,
32 when viewed using the Real-time Multivariate MJO index [Wheeler and Hendon 2004], which
33 includes lower and upper-tropospheric zonal winds in the MJO definition. Placing this activity
34 into a historical context, the YOTC MJO cases were weaker than those that occurred in 8 of the
35 previous 12 years, very much weaker than the very strong MJO activity that occurred in the
36 lead up to the 1997 El Nino, and a little weaker than the well-documented activity that
37 occurred during TOGA COARE (not shown).

¹ www.cpc.noaa.gov/data/indices/

² Mean and least-squares trend estimated for YOTC period from
ftp://ftp.cmdl.noaa.gov/ccg/co2/trends/co2_mm_mlo.txt

³ <http://www.swpc.noaa.gov/SolarCycle/>

1 Highlighting the more notable cases, the *May-June 2008 (a)* case involved modulation of
2 convective activity over much of the tropics, including an enhancement of convection over the
3 western Indian Ocean in late May (which approximately coincided with the start of the first
4 northward propagation of intraseasonal convection into India of the 2008 monsoon season
5 shown later in Figure 8), as well as an enhancement of convection in the eastern Pacific ITCZ
6 (as was associated with the development of several tropical cyclones (TCs)). The *April-May*
7 *2009 (d)* case included nearly 2 complete cycles of the MJO. The first exhibited strong
8 interaction with other equatorial waves (see first case in Section 3.2) and has been implicated
9 in the shift to El Niño conditions through the enhancement of westerly surface wind
10 anomalies across the Pacific (once convection reached the Pacific in late April). The second
11 cycle was associated with the first northward propagation of intraseasonal convection into
12 India for 2009 (see Figure 8). The *October-December 2009 (e)* case began with suppressed
13 convection over the near-equatorial Indian Ocean in mid October, followed by a switch to
14 enhanced convection over Africa and the western Indian Ocean which progressively gained in
15 strength until peaking in the second week of November with the strongest negative OLR
16 anomalies observed for the near-equatorial Indian Ocean for the whole of the YOTC period.
17 Finally, for the *December 2009-February 2010 (f)* case, enhanced convection reached further
18 eastward than any other MJO of the YOTC period, presumably helped by the warm Pacific
19 conditions. The MJO cases discussed above, including the nuances of their initiation,
20 propagation, possible connections, and influences on TC formation, make them excellent cases
21 for broadening our understanding of multi-scale interactions as well as for model verification
22 studies.

23 3.2 Convectively Coupled Equatorial Waves

24 Here we focus on just two periods of notable occurrences of CCEWs [Takayabu 1994;
25 Wheeler and Kiladis 1999; Kiladis et al. 2009]. The first case involves multiple interacting
26 waves during the period March-April 2009 (Figure 4; top). The MJO, ($n=1$) Equatorial Rossby
27 (ER), and Kelvin waves were all simultaneously active, seemingly propagating through each
28 other to account for the observed complex behavior of simultaneous eastward and westward
29 propagation. For example, the enhanced convection that occurred near 90°E on 10th April
30 appears to be a result of the superposition of the influence of all three waves propagating at
31 different speeds and/or directions. The ER wave in this example originates from an earlier
32 convective blow-up that occurred well to the east about 20 days previously. The Kelvin wave,
33 on the other hand, originates from the Atlantic, crossing 0°E on about the 2nd April. A later
34 strong Kelvin wave crossed the Atlantic and Africa in the first week of May.

35 The second case involves coherent westward movement of convection from east of the
36 dateline in the Pacific to the Indian Ocean during the month of March 2010 (Figure 4; bottom).
37 Consistent with the structure of an $n=1$ ER wave, this convection was mostly symmetric about
38 the equator and occurred in conjunction with cyclonic circulation cells on either side of the
39 equator. Imbedded within these cyclonic circulation cells were several TCs: TCs Tomas and
40 Ului in the southern hemisphere and TC Omais (Agaton) in the northern hemisphere. TC Ului
41 followed a long westward track, from $\sim 170^{\circ}\text{E}$ on 10th March to $\sim 150^{\circ}\text{E}$ on 21st March. In
42 addition, prominent Kelvin wave activity was observed during this case period (green
43 contours in Figure 4). These cases, and others like them, represent stringent tests for our
44 global models to properly represent and as yet little attention has been paid to the verification
45 of CCEW activity nor the metrics used for the evaluation (see M11).

1 3.3 Easterly Waves

2 As with the waves discussed above, easterly waves (EWs) play a key role in modulating
3 tropical cyclogenesis, and are most prevalent during the northern hemisphere summer over
4 West Africa and the tropical Atlantic [Reed et al. 1977; Kiladis et al. 2006] as well as the Pacific
5 [Reed and Recker 1971; Nitta and Takayabu 1985; Serra et al. 2008]. Figure 5 shows the July-
6 September variance of Tropical Rainfall Mapping Mission (TRMM) 3B42 precipitation rate
7 [Huffman et al. 2007] in the “tropical depression” (TD) wavenumber frequency band
8 (wavenumber -20 to -6 and period 2 to 5 days). Note that TCs may contribute to the TD-band
9 variance, especially in the western Atlantic and Pacific Ocean, north of 15°N. The top panel is
10 indicative of climatological EW storm tracks [Thorncroft and Hodges 2001]. The middle panel
11 shows that 2008 was characterized by anomalously high TD variance in the West African and
12 tropical Atlantic region. The region of maximum TD variance (6-15°N, 50°W-15°E) was 13%
13 higher in 2008 than climatology. In contrast, TD variance in 2009 was 5% lower than
14 climatology over the same region (Figure 5c). In 2008, TD variance was 20% below the 1998-
15 2009 mean over the region 6-15°N, 150-80°W. Anomalously low TD variance was especially
16 prominent in the Central Pacific consistent with the negative SST anomalies there (see Section
17 2). On the other hand, TD variance was 28% above climatology in 2009 over the same region
18 consistent with the presence of above average SSTs. Similarly, west Pacific TD-band variance
19 was also enhanced in 2009 [Hsu et al. 2009]. The relationship between the contrasting EW
20 activity in 2008 and 2009, ENSO, and ISV associated with the MJO and CCEWs including how
21 these vary with boundary forcings is an area of research that could benefit from the YOTC. It
22 will also be important and interesting to contrast the EW variability observed in the YOTC years
23 with that observed during the 2006 African Monsoon Multidisciplinary Analyses (AMMA) field
24 campaign over West Africa [Redelsperger et al. 2006; Janicot et al. 2008].

25 Figure 6 provides a more detailed look at the tracks and characteristics of easterly waves
26 during July-September 2008 and 2009. The Hovmöeller diagrams include precipitation rate
27 and objectively determined EW tracks based on 700 hPa vorticity maxima [Janiga 2010]. The
28 period between mid-July and early September 2008 was associated with numerous intense
29 African EWs moving over tropical North Africa into the East Atlantic. Consistent with past EW
30 composite studies [see Kiladis et al. 2006, and references therein] the peak precipitation rate
31 is located ahead of the EW tracks or in the northerlies over Africa (Figure 6). A closer
32 examination of the most intense waves reveals that mesoscale convective systems formed
33 northwest of the mid-level trough and then moved southwestward but remained fairly
34 coupled to the wave. One example of this is an EW that moved from the Ethiopian Highlands
35 to the East Atlantic between July 14th and July 22nd, 2008 (see dashed box in Figure 6a). Both
36 this wave and the preceding wave contributed to heavy rainfall and flooding in West Africa
37 with rainfall totals between July 17th and the 21st in excess of 4 cm over much of West Africa
38 and rainfall totals exceeding 10 cm in Burkina Faso and Liberia. Another high impact event
39 occurred on Sep. 1, 2009 (see dashed box in Figure 6b) when an mesoscale convective system,
40 tightly coupled to the mid-level trough of an EW, produced 263 mm of rainfall in
41 Ouagadougou, Burkina Faso according to rain gauges (not shown). Examinations of the
42 relationship between sub-synoptic aspects of the structure of the EWs and these convective
43 systems would be greatly aided by the high resolution of the YOTC analyses.

4 Tropical Cyclones

Tropical cyclones (TCs) are by far one of the most significant manifestations of organized tropical convection, notably because of their sheer elegance as a physical system but also because of the societal need for ever-increasing accurate predictions of their strength and track. Climatologically speaking, the last several years have been remarkably below average in terms of overall global tropical cyclone activity. Since the previous peak in overall global and Northern Hemisphere Accumulated Cyclone Energy (ACE) in 2005, tropical cyclone activity has significantly decreased especially over the entire Pacific with the 2008-09 YOTC “year” having the lowest global ACE since 1977 [Maue 2009, 2011]. Despite YOTC occurring within a historically quiet period relative to the last three decades, there were still ample TCs that developed, with some particularly unique cases and conditions.

The tracks of all TCs during the YOTC period are illustrated in Figure 7, with those mentioned below annotated with a number at the start and end of the track. In 2008, the western North Pacific had 25 tropical storms with 12 becoming typhoons - a season with slightly below normal activity. Typhoon Jangmi (Figure 7a – track 1) was the strongest TC of the season across the whole northern hemisphere with sustained winds of 145 knots. Unusually, Japan received no direct landfalls during this season. The eastern North Pacific exhibited activity close to normal. Hurricane Norbert (Figure 7a – track 2) was the strongest of the season and was also one of three (with Julio and Lowell) to make landfall over Mexico. The North Atlantic was active; for the first time, major hurricanes (winds 100 knots or more) occurred in each of the five consecutive months from July to November. Hurricanes Fay, Gustav, Ike and Paloma all hit Cuba. Ike (Figure 7a – track 3) was one of the largest storms (in aerial size) ever recorded in this basin and caused a storm surge of up to 7m along the Gulf coast. In the North Indian Ocean, the most significant storm was Cyclone Nargis (Figure 7a – track 4), which made landfall over Myanmar and caused a huge storm surge up the Irrawaddy delta. This resulted in the loss of as many as 100,000 lives. During the 2008-9 southern hemisphere season four storms brought heavy rainfall to Madagascar. Cyclones Dominic and Ellie (Figure 7b – tracks 1 and 2) made landfall over the Australian coast whilst the strongest storm of the season, Hamish (Figure 7b – track 3) kept just offshore of the Australian east coast.

During the 2009 northern hemisphere season the El Niño induced stronger typhoons in the western North Pacific and the storm tracks tended to originate further east into the central parts of the Pacific Ocean. The strongest typhoon of the season, Nida (Figure 7a – track 5), peaked with sustained winds of near 160 knots. Notable events were Typhoon Ketsana (Figure 7a – track 6) that caused extensive flooding in the Philippine capital Manila and later across Vietnam and Cambodia and slow moving Typhoon Parma (Figure 7a – track 7) that dumped an estimated 1.8 m rain over the northern Philippines. The El Niño also resulted in higher than normal activity in the eastern and central North Pacific. Hurricane Rick (Figure 7a – track 8) became the second strongest east Pacific hurricane on record, making landfall over Mexico, as did Hurricane Jimena (Figure 7a – track 9). In the North Atlantic, the El Niño resulted in a quiet season for the Caribbean and United States. The most unusual event of the season was high latitude tropical storm Grace (Figure 7a – track 10) that developed near the Azores and eventually tracked across the United Kingdom as an extra-tropical system. In the North Indian Ocean, tropical storm Aila (Figure 7a – track 11) caused a storm surge of up to 3m across Bangladesh that resulted in hundreds of fatalities in this region. The most notable events for the 2009-10 southern hemisphere season included tropical storm Hubert (Figure

1 7b – track 4) that caused significant disruption over Madagascar. While activity was quiet
2 around Australia, several storms [Laurence, Magda, Olga and Paul (Figure 7b – tracks 5, 6, 7
3 and 8)] impacted coastal regions. Mick and Tomas (Figure 7b – tracks 9 and 10) both affected
4 Fiji and Ului (Figure 7b – track 11) was the strongest South Pacific cyclone for five years. To
5 round off the season, a highly unusual tropical storm in the South Atlantic developed in March
6 2010 and was named Anita by Brazilian meteorological organizations (not shown). It was the
7 first such storm to develop in this region since Catarina in 2004, although unlike Catarina
8 posed no threat to land.

9 TC research in YOTC benefits from the occurrence of the THORPEX-Pacific Asian
10 Regional Campaign (T-PARC) and Tropical Cyclone Structure-2008 (TCS-08) field
11 experiments that conducted multiple aircraft operations into Typhoons Nuri, Sinlaku, Hagupit,
12 and Jangmi. The science objectives of these campaigns included increasing understanding of
13 TC formation, structure and intensity change, extratropical transition, and the value of
14 targeted observations. In particular, analysis of aircraft observations are being conducted
15 with reference to gridded YOTC analyses fields provided by the European Centre for Medium-
16 Range Weather Forecasts (ECMWF).

17 **5 Monsoons**

18 The monsoons exhibit considerable breadth in terms of the phenomena and range of
19 space and time scales associated with tropical convection [e.g., Ramage 1971; Murakami
20 1975; Gadgil 1981; Lau and Lim 1982; Hastenrath 1987; Trenberth et al. 2000; Rodwell and
21 Hoskins 2001; Wang 2006]. This includes seasonal and planetary-scale changes in the
22 atmospheric and ocean circulations, a preponderance of tropical wave activity, modulations of
23 TCs other synoptic scales, and diurnal variations. The monsoons represent highly integrating
24 features of tropical convection, and remain an ominous forecast challenge from not only their
25 onset, but for subsequent breaks and active periods, extreme events and seasonal totals. Here,
26 we highlight some of the notable monsoon characteristics during the YOTC period.

27 *5.1 Indian*

28 With the 2008 Indian summer monsoon being “normal”, garnering 98% of long-term
29 average all India rainfall (AIR), and 2009 being one of the worst drought over the past century
30 with AIR being 22% below the long term average, the YOTC period provides a unique
31 opportunity to examine and unravel differences in propagation characteristics and structure
32 of the monsoon intraseasonal oscillations (MISOs) and how they lead to interannual
33 variability. Evolution of the daily rainfall over India (between 72E-85E, 6N-27N) indicates
34 (Figure 8) that the near-normal monsoon of 2008 had three strong, active spells of rainfall
35 and only two weak breaks, while the severe-drought monsoon of 2009 was characterized by
36 three long breaks and two weak active spells. This is consistent with some recent studies
37 [Joseph et al. 2009] indicating that long breaks are characteristic features of Indian monsoon
38 droughts. The monsoon onset over Kerala (MOK) during 2008 occurred on 31 May, close to
39 the climatological date. Although 2009 was a drought year, the onset took place on 23 May, a
40 week before the normal onset date consistent with earlier findings that MOK has no
41 relationship with the performance of the monsoon.

42 Significant differences in ISV during 2008 and 2009 are noteworthy (Figure 8 c- f). The
43 time-latitude diagrams of 30-60 day filtered OLR anomalies averaged over Indian longitudes
44 show that the northward propagation of MISO was slower during 2008 compared to that

1 during 2009. Also, consistent with the daily rainfall (Figure 8 a-b), the MISO during 2008 was
2 characterized by three wet and two dry northward propagating spells while during 2009
3 there were two wet and three dry spells. Another important feature (Figure 8 b and d) is the
4 intensity of the long break during August 2009 that contributed to the severity of the drought
5 of the year. What was responsible for this intense long break during 2009? Neena et al [2011]
6 show that an interaction between a westward propagating planetary-scale equatorial Rossby
7 wave and the northward propagating MISO may have been responsible for this intense long
8 break. The characteristic spatial pattern associated with the MISO during the two years also
9 had notable differences. Regressed 10-90 day filtered OLR and winds at 850 hPa with respect
10 to a reference time series (filtered OLR averaged over central India) shows a canonical
11 convectively coupled monsoon ISV structure with a meridional dipole in OLR over Indian
12 longitudes during 2008 [Waliser 2006; Goswami 2011]. During 2009, the meridional dipole
13 structure of convection is conspicuously absent, leading to a much larger meridional scale for
14 low level winds during 2009 compared to 2008. Understanding what is responsible for the
15 differences in propagation characteristics and spatial structure of ISV between these two
16 years is crucial for developing the ability to forecast them at lead times of 2-3 weeks, and is a
17 major challenge for YOTC.

18 **5.2** *East Asian / Western North Pacific*

19 As with the Indian monsoon, the July-September seasonal-mean low-level circulation
20 and convective activity in the East Asian/Western North Pacific (EA/WNP) monsoon region
21 were distinctly different between 2008 and 2009. During July-September 2008, the monsoon
22 trough was weaker than normal and confined mostly in the South China Sea, while the ridge
23 was unusually strong and occupied the whole western North Pacific (WNP) from the equator
24 to 50°N (Figure 9). Rainfall was above normal for most of the WNP, and in particular in the
25 tropics from the South China Sea all the way to the Dateline. The stronger monsoon trough
26 and more rainfall were likely induced by the 2009 El Nino, which became mature in early
27 summer [e.g., Lau and Nath 2006]. In contrast, the monsoon trough was stronger and
28 extended further eastward than normal in July-September 2009, while the ridge shifted more
29 northward than usual. The corresponding circulation was characterized by a cyclonic anomaly
30 in the South China Sea and the Philippine Sea and anticyclonic anomaly in the extratropical
31 WNP. Moreover in 2009, the tropical EA/WNP from the South China Sea to 150°E was
32 dominated by a westerly anomaly. As a result, rainfall was above normal for most of the WNP,
33 and in particular in the tropics from the South China Sea all the way to the Dateline.

34 Percentile maps show how anomalous the rainfall and specific humidity were during
35 YOTC. The 850-hPa specific humidity was generally above the 85th percentile in the WNP
36 west of 140°E, but lower than the 15th percentile east of 160°E in the prevailing region of the
37 unusually strong subtropical ridge. Extremely low rainfall (below the 10th percentile) was
38 observed in the region between 5°N-15°N and east of 140°E where the anticyclonic circulation
39 and easterly anomaly prevailed. In July-September 2009, the high specific humidity region
40 extended further eastward and occupied almost the whole tropical and subtropical EA/WNP
41 region. While rainfall was above the 50th percentile throughout most of this region, it was
42 generally not as extreme as in specific humidity, except in the central rainfall-abundant areas
43 where it exceeded 90 percentile. Extremely low rainfall was found east of Taiwan and south of
44 Japan and in the subtropical WNP east of 160°E, in all cases where the anticyclonic anomalies
45 prevailed. Note that typically July-September rainfall in the WNP is largely contributed by

1 tropical cyclones, and this appears to be the case for the rainfall and TC distributions in 2008
2 and 2009 (see Figure 7). The characteristics above emphasize the multi-scale nature of
3 tropical convection and the interactions between synoptic and finer scale convection, the
4 large-scale circulations (e.g, monsoons and CCEWs) and basin-scale climate (e.g., ENSO).

5 5.3 *Australian*

6 The YOTC period covers two wet seasons in northern Australia, which occur in austral
7 summer. Figure 10 shows a daily time series of rainfall together with the climatological rainfall
8 distribution at Darwin (blue line). Significant intraseasonal variability is exhibited, some of
9 which may be attributed to the MJO (see Section 3.1). However, tropical cyclones also
10 contributed significantly to Darwin rainfall, namely TC Billy (Dec 2008), TC Lawrence (Dec
11 2009) and ex-TC Paula (Mar 2010) (see Section 4; Figure 7), as did a monsoonal low during
12 late February 2010 and long-lived continental squall lines during late October 2009.

13 Through the development of an objective technique to better characterize the state of
14 the north Australia wet season on any given day, Pope et al. [2009] showed that it is important
15 to consider the entire wet season rather than just the embedded shorter monsoon period.
16 This is because a significant fraction of the rainfall occurs outside the traditionally defined
17 monsoon period. The state analysis technique involved the identification of five wet-season
18 regimes from daily radiosonde data at Darwin. Three of the regimes, termed Deep West, Moist
19 East and Shallow West are typically associated with rainfall, where Deep West identifies the
20 active phase of the monsoon and Moist East signifies monsoon build-up, break and retreat
21 conditions. Two of the five regimes (East and Dry East) represent generally dry conditions.
22 The wet season onset can be identified by the first significant consecutive days of the Moist
23 East Regime and monsoon onset is related to the first occurrences of the Deep West regime.
24 Likewise the retreat of the monsoon and the end of the wet season can be determined as the
25 last days of the Deep West and Moist East regimes respectively. Figure 10 shows the daily
26 identification of wet-season regimes as described above for the two north Australia wet
27 seasons within YOTC. Also shown are the climatological monsoon onset and retreat days
28 (vertical dashed lines) and the monsoon onset and retreat days for the two seasons (arrows).

29 Using the Moist East regime as an indicator, the 2008-09 wet season started in early
30 November and lasted until mid March. In contrast, the 2009-10 wet season started in early
31 December and lasted well into April. This is consistent with La Niña conditions in 2008-09,
32 which promote an early wet-season onset [Nicholls et al. 1982; Drosowsky 1996], while the
33 slight El Niño in 2009-10 favored a later wet-season onset. Using the definitions above, the
34 onset in 2008 and 2009 occurred on December 18, 2008 and December 15 2009, respectively,
35 close to the mean onset date December 19 [Pope et al. 2009]. The retreat of the monsoon
36 occurred on February 17 2009 and March 5 2010, respectively. Hence, the 2008-09 monsoon
37 season was relatively short, while the 2009-10 season was of more or less average length, and
38 the wet season as whole lasted significantly longer than in 2009/10 than 2008/09.

39 5.4 *N. American*

40 By measures such as all-Mexico June-August total rainfall, the 2008 North American
41 Monsoon (NAM) was the largest since 1941. Positive rainfall anomalies in gauge data (not
42 shown) and negative peak season (Jul-Aug) OLR anomalies (Figure 11a) were exhibited in
43 nearly all regions of Mexico and throughout much of the US-Mexico border region. Consistent
44 with previous studies [Higgins et al. 1998; Castro et al. 2001; Gochis et al. 2007] [Liebmann et

1 al. 2008], antecedent SST conditions appear to have played a significant role in the
2 development of this anomaly. Weakening wintertime La Niña conditions (Figure 11c and
3 Figure 1) in the central and western Pacific, and an extended wintertime drought and warm
4 surface temperatures over western Mexico and the Southwest US, helped initiate an early,
5 robust onset to the NAM in mid-to-late June. Regional precipitation tracking indices developed
6 as part of the NAM Forecast Forum [Gochis et al. 2009] showed all NAM regions, experiencing
7 anomalously high precipitation accumulations through July. Persistent diabatic heating from
8 convective activity (inferred from negative OLR anomalies) and a northwestward shift in the
9 200mb height field (Figure 11e) during July and August helped provide a favorable pattern for
10 sustained low-level moisture advection (not shown) from the Gulf of California, tropical
11 Eastern Pacific and the Gulf of Mexico into the NAM region [Higgins et al. 2004]. As mentioned
12 in Section 4, owing to favorable steering circulations, land-falling and near shore tropical
13 storms also made significant contributions to rainfall totals during July-September of 2008.
14 Englehart and Douglas [Englehart and Douglas 2001], Wang et al. [Wang et al. 2008] and
15 Serra [Serra 2009] each note that circulation patterns favorable for sustaining NAM rainfall
16 are also likely to steer tropical storms into Mexico, the Southwestern US, Baja California and
17 the Texas Gulf Coast. Thus, for a year like 2008, both the large-scale circulation and episodic
18 extremes appear to have contributed to the record rainfall totals.

19 In contrast to 2008, seasonal changes in Pacific sea surface temperatures towards
20 moderate El Niño conditions by summertime appeared to have had a significant impact on the
21 2009 NAM (Figure 11d). While the onset of the 2009 NAM was over a week early compared to
22 climatology, the overall monsoon circulation pattern and its associated rainfall deteriorated
23 substantially by late July. Consequently, Jul-Aug OLR anomalies (Figure 11b) were mostly
24 positive over the southwest US and Mexico. A number of areas of Mexico experienced some of
25 the worst seasonal drought in recent history. Similarly, parts of western Arizona and the
26 broader regions of the lower Colorado River valley experienced rainfall totals approaching
27 only 50% of normal. Previous studies, cited above, have shown that El Niño conditions can
28 suppress NAM rainfall, particularly over southern and eastern Mexico, by enhancing
29 convection in the Eastern Pacific ITCZ, reducing the northward transport of moisture and
30 contributing to a poorly developed monsoon ridge structure, evidenced by the 200mb height
31 anomalies in Figure 11f, and a weakened overall monsoon circulation [Cavazos and
32 Hastenrath 1990; Gochis et al. 2007]. Related to this weaker than normal circulation pattern,
33 was a less than normal occurrence of tropical storm landfall and near-shore activity in both
34 eastern and western NAM regions during 2009 (Figure 7). The strong evolution in large scale
35 SST forcing and associated tropical activity during the YOTC appears to have had a significant
36 impact on the timing (onset), intensity and total accumulation of N. American monsoon
37 rainfall. However, seasonal forecasts had difficulty in both years predicting such impacts,
38 highlighting the need for continued work in understanding large-scale ocean-monsoon
39 interactions in N. America.

40 5.5 S. American

41 The South American monsoon (SAM) region extends from Southern Amazonia and the
42 upper Parana-Basin, and various studies have identified its characteristics and variability in
43 various time scales [Ramage 1971; Zhou and Lau 1998; Vera et al. 2006; Liebmann et al. 2007;
44 Marengo et al. 2010]. The “mature” phase of the monsoon in the SAM region occurs during
45 the warm season December-February, with the onset of the rainy season between September-

1 November and the demise occurring after May (See Marengo et al 2010 and references quoted
2 in). The climatological onset of the SAM ranges between mid October to early November,
3 depending on the definition [Liebmann and Marengo 2001; Carvalho et al. 2011; Nieto-
4 Ferreira and Rickenbach 2011], with the mean demise occurs in early May, and with both the
5 onset and demise dates exhibiting interannual variability. Key variability influencing the
6 onset and demise, as well as the strength and evolution of the SAM, are the South Atlantic
7 Convergence Zone (SACZ) and the South America Low Level Jet (SALLJ) East of the Andes.
8 Variations in the former have been found on intraseasonal to interdecadal time scales
9 [Nogues-Paegle and Mo 1997; Grimm and Zilli 2009; Grimm 2010], and often exhibit a dipole
10 structure in rainfall between the SACZ and the subtropical plains just to the south. A
11 strengthening of the SALLJ typically accompanies the suppressed SACZ – wet subtropical
12 plains phase of the dipole, which transports massive amounts of moisture from the Amazon
13 Basin into the sub-tropics [Silva and E. H. Berbery 2006]. In addition, strong SALLJ events are
14 linked to short-term extreme precipitation events in the plains of central Argentina
15 [Liebmann et al. 2004; Salio et al. 2007]. On the other hand, a SACZ-enhanced phase induces
16 extreme heat waves over the sub-tropical regions [Cerne and Vera 2010].

17 For the YOTC period, rainfall in the Sep–Nov2008 onset phase was below average over
18 central-southern Brazil and most of Argentina (deficit exceeding 200 mm), with above normal
19 rainfall over northern Amazon Basin and portions of southern Brazil (Figure 12A). In the
20 mature phase, Dec 2008-Feb 2009 (Figure 12B), rainfall was below average over the SAM
21 region and in southern Brazil and most of Argentina, with anomalies greater than 270 mm.
22 Above average rainfall was observed over the northern Amazon Basin and Northeast Brazil,
23 with anomalies larger than 200 mm. During the decay phase, Mar-May 2009, well above-
24 average rainfall was observed over northeastern Brazil and northern Amazonia (Figure 12C).
25 This is attributed to the anomalously warm Tropical South Atlantic Ocean and a southward
26 position of the ITCZ that usually moves northward in April, but stayed in place until May. This
27 resulted in anomalously strong moisture transport from the tropical Atlantic into the Amazon
28 region. At this same time, La Nina conditions were evident in the tropical Pacific, which
29 typically intensify the upward branches of the Walker and Hadley cells over Amazonia, and
30 lead to abundant precipitation conditions. As a consequence of the intense rainfall, the
31 Amazon basin exhibited heavy flooding, with water levels higher than in several decades. In
32 July 2009, the levels of the Rio Negro in Manaus reached 29.75 m, a new record high since the
33 beginning of data collection in 1903. This resulted in over 300,000 people left homeless and
34 40 fatalities because of the floods [Marengo et al. 2011a]. Another factor contributing to the
35 intense rainfall in Northeast Brazil during this season was the active MJO (See Figure 3; Note
36 active MJO in eastern hemisphere, wide latitude averaging cancels signal out in this diagram
37 over S. America).

38 For the 2009-2010 monsoon season, warm SST conditions prevailed in the Pacific.
39 During the onset season (Figure 12D), negative rainfall anomalies were widespread, with
40 dryer conditions persisting from northern Amazonia to Venezuela. This is attributed to an
41 anomalous northward displacement of the ITCZ induced by warm surface waters in the
42 tropical North Atlantic. Above-average rainfall was observed over parts of southern Brazil
43 (about 280 mm above normal) and Paraguay, in association with increased frontal
44 activity. During the mature phase, Dec 2009-Feb 2010 (Figure 12E), rainfall totals were near
45 average over the southern Amazon basin, and slightly below-average over central Brazil and
46 the north-central Amazon basin. Above-average rainfall was observed over southern Brazil,
47 northeastern Argentina, Uruguay and extreme northeastern Argentina, while below average

1 rainfall was observed over most of eastern Brazil. During March and April (Figure 12F),
2 rainfall totals were below average over central Brazil and Northeast Brazil and above average
3 over Northeast Brazil. During this period, Equatorial SSTs were 0.5°C - 1°C above average
4 across the eastern Pacific, and 0.5°-1.5°C above average in the equatorial Atlantic, west of
5 10°W. This facilitated a northward migration of the ITCZ with dry conditions in Northeast
6 Brazil and tropical South America east of the Andes, leading to one of the most intense
7 droughts in Amazonia during the last 107 years [Marengo et al. 2011b].

8 5.6 West Africa

9 The year-to-year variability of Sahel rainfall, and thus the west African monsoon, is of
10 great interest due to the very strong north-south gradient in natural and anthropogenic
11 conditions. Figure 13 shows that both 2008 and 2009 May-September seasons were slightly
12 wetter than the long-term average, consistent with a recent wet trend in this region [Fink et
13 al. 2010]. Further scrutiny illustrates that the anomalously wet Sahel signal in both years was
14 mainly exhibited in the western Sahel west of about 0°E. The wet West Sahel in 2008 was part
15 of a regional-scale wet anomaly that covered most of the West African region down to the
16 Guinea Coast. Other notable anomalies in 2008 included a drier (wetter) than normal Sudan
17 (Ethiopian highlands). While the West Sahel was also wet in 2009, the West African region as
18 a whole was drier compared to climatology, with notable dry anomalies in Liberia and the
19 Ivory Coast, in much of Nigeria, and most prominently (compared to 2008) in the Sudan and
20 Chad regions. The more widespread dry anomalies seen in 2009 compared to 2008 are
21 consistent with the developing El Nino (Figure 1). In addition, the relatively dry Guinea Coast
22 and wet Sahel would classify the 2009 season as a “dipole year” [Ward 1998], which is
23 consistent with the observed cooler equatorial Atlantic during summer 2009 compared to
24 2008 (Figure 1)

25 West African monsoon onset and within-season rainfall variability, including their
26 predictability, have received particular attention in recent years due to their obvious societal
27 impacts [e.g., Sultan and Janicot 2000]. The YOTC dataset should be exploited to establish the
28 extent to which these can be understood and explained in terms of dynamical processes such
29 as inertial instability [e.g., Sultan and Janicot 2003; Hagos and Cook 2007; Nicholson and
30 Webster 2007] or thermodynamic processes associated with variations in the Atlantic cold
31 tongue [e.g., Okumura and Xie 2004], the Saharan heat low [e.g., Ramel et al. 2006], influences
32 by ISV, including the MJO [Janicot et al. 2008; Barlow 2011] and the passage of CCEWs. An
33 important component of west African monsoon variability is the presence of well-defined
34 synoptic EWs, which account for 25-35% of the total variance of deep convection [e.g., Mekonnen
35 et al. 2006]. This suggests a need to improve our understanding of the two-way interactions
36 between the EWs (see Section 3.3 above) and the regional environment in order to better
37 understand variability in the monsoon as well as the downstream tropical Atlantic.
38 Comparing figs. 5 and 13 highlights the fact that the 2008 season was characterized by more
39 EW activity and was generally wetter than in 2009, suggesting a potential relationship
40 between the EW activity and seasonal rainfall. Studies indicate that EW activity can be
41 influenced by rainfall modulation in the EWs themselves [Hsieh and Cook 2005, 2007],
42 stability of the African easterly jet [e.g., Leroux and Hall 2009], triggering by tropical
43 convection [e.g., Thorncroft et al. 2008; Leroux et al. 2010], and triggering by extratropical
44 troughs [Leroux et al. 2011]. The YOTC dataset should be exploited to ascertain the relative
45 roles of these factors. Finally, it is now well known that Kelvin waves can significantly

1 modulate rainfall and can both trigger and intensify EWs [e.g., Mekonnen et al. 2008; Ventrice
2 et al. 2011]. Figure 4 highlights the presence of Kelvin waves in spring when they are known
3 to be important in the equatorial African region [Nguyen and Duvel 2008] but are also known
4 to influence the Guinea coastal region of West Africa (not shown). Two notably strong Kelvin
5 wave events occurred in early May 2008 and should be strong candidates for study in the
6 YOTC dataset.

7 **6 Tropical – Extratropical Interactions**

8 *6.1 Extratropical transition of tropical cyclones*

9 During extratropical transition (ET), tropical cyclones undergo significant structural
10 changes, especially with regards to the distribution of deep convection, clouds and
11 precipitation [Jones et al. 2003]. The interaction with the midlatitude flow during ET can lead
12 to the excitation of a Rossby wavetrain [Harr and Dea 2009] and thus impact the midlatitude
13 weather and predictability far from the location of the ET event [Anwender et al. 2008; Harr et
14 al. 2008] (see also M11). A primary objective of the THORPEX Pacific Asian Regional
15 Campaign (T-PARC), that took place during the YOTC period, was to increase understanding of
16 the impact of tropical cyclone structure on the ET process and subsequent midlatitude
17 downstream development.

18 A unique set of observations of the structural changes during the ET of Typhoon Sinlaku
19 (2008) was obtained during T-PARC. Following recurvature, Sinlaku was significantly altered
20 by strong vertical wind shear from the west. The vortex core was tilted toward the east and
21 the low-level circulation center was fully exposed as deep convection was suppressed. As the
22 decaying Sinlaku approached southern Japan, several episodes of deep convection erupted to
23 the east and downshear of the circulation center. The tropical cyclone re-intensified to
24 typhoon strength with a circulation center co-located with new episodes of the deep
25 convection. *In situ* measurements obtained by T-PARC documented how the characteristic
26 monopole vorticity structure evolved to a low-level center associated with the original
27 tropical cyclone and a new vorticity center to the northeast, located in the region of the
28 episodes of deep convection. Analysis of convective and stratiform precipitation from YOTC
29 ECMWF analyses defined the presence of both cloud types in the region of the new vorticity
30 maximum. Therefore, the diabatic fields indicate a tropical mesoscale circulation system with
31 a stratiform region downstream from a leading convective cell. The re-intensification period
32 resulted in a stronger intensity and modified structure of Sinlaku as it eventually underwent
33 ET, and thus had an impact on its interaction with the midlatitude flow. During and following
34 the ET a small-scale Rossby wavetrain developed and appeared to interact with a larger-scale
35 midlatitude Rossby wavetrain (Figure 14c) No Rossby wavetrain is seen downstream of the
36 second T-PARC ET case, Typhoon Jangmi. However, the divergent outflow from Jangmi
37 appeared to accelerate a midlatitude jet streak.

38 During the YOTC period, low predictability, identified as increased standard deviation in
39 the 3, 5 and 7 day forecasts of the ECMWF ensemble prediction system (EPS), is particularly
40 marked when a clearly defined Rossby wavetrain develops or amplifies directly downstream
41 of an ET event. This is seen for the ET of Halong in May 2008 (Figure 14a,b), Bavi in October
42 2008 (Figure 14c) and a further seven examples in the western North Pacific, two in the North
43 Atlantic and three in the Southern Hemisphere. In contrast, following the ET of Rammasun
44 (Figure 14a,b), ridging occurs downstream of the ET but the Rossby wavetrain does not

1 amplify until it reaches the eastern North Pacific. The EPS spread also increases at this stage.
2 Similar behavior was seen in two other cases during the YOTC period. For Nakri in 2008
3 (Figure 14a,b) and five Southern Hemisphere ETs, the main signal is a midlatitude Rossby
4 wavetrain that is not modified during ET and exhibits weak to moderate EPS spread.

5 The YOTC period offers cases both of structural changes during ET as well as a variety of
6 interactions between ET systems and the midlatitude flow. A priority for research with the
7 combination of YOTC data sets and T-PARC observations will be to quantify the role of
8 structural changes of the tropical cyclone before and during ET (e.g., increased outflow at
9 upper levels, increased heat and moisture transport to midlatitudes) on the downstream
10 midlatitude predictability (see M11).

11 6.2 *Extratropical Influences on the Tropics*

12 Upper-level disturbances penetrating from the extratropics into the subtropics and outer
13 tropics can significantly influence the weather [e.g., Knippertz 2007 and references therein]
14 and wave activity in the tropical belt, including Kelvin waves [e.g., Straub and Kiladis 2003],
15 mixed-Rossby gravity waves [e.g., Magana and Yanai 1995] and the MJO [e.g., Weickmann et
16 al. 1985; see review by Roundy 2011]. The eastern tropical Atlantic and Pacific Oceans and the
17 adjacent landmasses are frequently affected by such tropical–extratropical interactions. As an
18 example, we focus on West Africa, where upper-level disturbances regularly trigger moderate
19 precipitation events during the boreal-winter dry season [Knippertz and Fink 2008, 2009].
20 These significant anomalies can lead to high impacts on the affected population (e.g., rotting
21 harvests, improved Mango yield and grazing conditions, locusts). In extreme cases, heavy
22 precipitation, flooding, destruction of infrastructure, and loss of lives can occur [Knippertz
23 and Martin 2005; Meier and Knippertz 2009].

24 During the two dry seasons of the YOTC period five significant West African wet
25 episodes occurred: 05–06 December 2008, 08–09 January 2009, 16–19 February 2009, 31
26 October–01 November 2009, and 12–14 December 2009. Here we will briefly discuss the
27 February 2009 case as an illustration of the phenomenon [Knippertz and Fink 2008, 2009].
28 Figure 15a shows accumulated precipitation from over the four-day February 2009 period.
29 Heavy precipitation occurred over northern Ivory Coast, southeastern Guinea and southern
30 Mali, with light precipitation extending across the Sahel far into the southern Sahara. These
31 rainfalls were preceded by a wave-breaking event over the North Atlantic that generated a
32 trough with a strongly positive tilt in the horizontal over Morocco and Algeria on 16 February
33 2009 (marked in figure). Tight gradients in the geopotential at 300 hPa all across northern
34 Africa indicate a subtropical jet streak. The mean sea-level pressure (MSLP) falls significantly
35 to the southeast of the trough (i.e., in the right entrance region of the jet streak), leading to a
36 northward shift of the weak wintertime heat low to eastern Burkina Faso on 16 February
37 2009 (“X” in figure), 5° to the north of its climatological position. The associated enhanced
38 north–south MSLP gradient at its equatorward flank allows moist air from the Gulf of Guinea
39 to penetrate farther than usual into the continent and feed the rainfall. The upper-trough
40 drifts southwestward along the northwest African coast until 19 February while the surface
41 low slowly weakens (not shown). The resulting rainfall is mainly related to rather short-lived
42 cellular convection during the afternoon and evening of 16–18 February and a slightly more
43 organized system in the early morning hours of 19 February. These systems occur at the
44 southern end of an extended southwest–northeast-oriented cloud band [a so called ‘tropical
45 plume’, see Knippertz 2007], which drifts very slowly westward during 16–20 February in

1 connection with the movement of the upper-trough (Figure 15c). A vertical cross section
2 through this plume showing Cloudsat radar reflectivity (Figure 15d) indicates a sudden
3 south–north decrease in cloud top height and three bands of precipitation. Strong evaporation
4 at low levels, however, inhibits significant accumulations (Figure 15a).

5 Consistent with results by Knippertz and Fink [2009], the general northward shift of the
6 rain zone was reasonably well predicted with five day leads by the ECMWF. Despite this, the
7 relative contributions of dynamical versus diabatic processes to the pressure fall are not well
8 understood [Knippertz and Fink 2008], and details of the associated moisture inflow from the
9 Gulf of Guinea and the ensuing tropical convection challenge present-day forecast models.
10 Note the synergistic use of the high resolution ECMWF YOTC analyses, station measurements
11 and satellite data to develop a robust characterization of this multi-faceted and impactful
12 event – a capability that YOTC objectives are focused on facilitating (see M11).

13 6.3 Atmospheric Rivers

14 Atmospheric rivers (ARs) are narrow channels of enhanced atmospheric moisture
15 transport that play a key role in the tropical-extratropical water cycle. Occupying ~10% of the
16 earth’s circumference in the midlatitudes, they account for over 90% of the poleward
17 moisture transport [Zhu and Newell 1994, 1998]. They largely form in the extra-tropical
18 ocean basins north of the tropical moisture reservoir. Some ARs are more directly linked to
19 the tropics with moisture supplied by the “tropical plumes” while some ARs show more of a
20 subtropical or mid-latitude moisture source [e.g., Ryoo et al. 2011]. Landfalling ARs often lead
21 to enhanced precipitation in the mountains of the west coast of North America, and are
22 responsible for some extreme precipitation/flood events in the region [Ralph et al. 2006;
23 Neiman et al. 2008a]. Detection of ARs involves identifying narrow channels of enhanced
24 moisture, typically identified in satellite observations of integrated water vapor (IWV) [Ralph
25 et al. 2004; Neiman et al. 2008b]. For this overview of the ARs during YOTC, daily maps of IWV
26 from the Atmospheric InfraRed Sounder (AIRS) were manually examined for AR-like
27 structures (i.e., moisture plumes with 2 cm or greater IWV, narrower than 1000 km and
28 longer than about 2000 km; [Ralph et al. 2004]). Approximate locations of the ARs identified
29 are shown in Figure 16 for the two half periods (i.e. years) of YOTC.⁴ A total of 259 ARs are
30 identified, with 122 and 137 during each half period. In the first year, the maximum number of
31 ARs occurred in the northeastern Pacific, with a similar number observed there in the second
32 year. The southeastern Pacific, on the other hand, saw an increase of 70% in the number of
33 ARs in the second year. This is likely to be an influence of ENSO but the manner this may be so
34 has not been established. Noteworthy is the scarcity of landfalling ARs in California during the
35 YOTC period, as the average occurrence is about 15 per year [Neiman et al. 2008b]. It is also
36 worth noting that the “tropical plume” events/wet episodes over West Africa discussed in the
37 previous subsection were not associated with ARs according to the IWV threshold

38 The impact of landfalling ARs is illustrated in Figure 17 with an example of an extreme
39 precipitation event in California’s Sierra Nevada mountains. There, a few AR events can result
40 in as large as 40% of the total seasonal snow accumulation [Guan et al. 2010] —an important
41 water resource during summer. The figure shows the IWV plume and the 3-day cumulative

⁴ AIRS data are not available during 10–25 January 2010 due to hardware failure. AR detection was not performed for that period.

1 precipitation associated with this event, which reached 9 cm on average⁵. A number of studies
2 have showed the connection of the MJO to precipitation extremes in the US West Coast and
3 elsewhere [Mo and Higgins 1998a, 1998b; Jones 2000; Bond and Vecchi 2003]. Ralph et al.
4 [2011] showed an interesting case in which the development of a high-impact AR that made
5 landfall over the Pacific Northwest was favored by MJO convection over the eastern Indian
6 Ocean and equatorward Rossby wave energy propagation. Analysis of snow accumulation in
7 the Sierra Nevada showed a preference of AR-related extreme events to occur when MJO
8 activity is enhanced in the far western Pacific [Guan et al. 2010]. Three AR-related extreme
9 precipitation events during YOTC (including the one discussed here) occurred during
10 relatively weak MJOs (amplitude ≤ 1) in the Indian/Western Pacific Oceans. It remains to be
11 explored and understood how conditions in the tropics (such as convection and circulation
12 anomalies associated with MJO and ENSO) and tropical-extratropical interactions affect the
13 formation and impact of ARs. The complexity of the multi-scale interactions involved in such
14 processes, as illustrated in Ralph et al. [2011], is of crucial interest to YOTC
15

⁵ Three high-impact (3-day cumulative precipitation > 9 cm in the Sierra Nevada) AR events in California were identified during the YOTC period. However, none of them strictly conformed to the Ralph et al. criteria in terms of length or overall structure, including the one discussed here which was 5% shorter than the criteria and thus isn't included in Figure 16. On the other hand, three ARs meeting the criteria were identified in California during YOTC, but all with low impact (3-day cumulative precipitation < 0.5 cm in the Sierra Nevada).

SIDEBAR: Shallow Convection Processes: A VOCALS and YOTC Overlap

Understanding shallow convection processes is critical to achieving better simulations and predictions associated with the expansive, low-level, high-albedo cloud regions of the tropics as well as of transitions between shallow and deep convection. A primary goal of the Variability of the American Monsoon Systems (VAMOS) Ocean-Cloud-Atmosphere-Land Study (VOCALS) Regional Experiment (REx) is to characterize the structural properties of the marine boundary layer (MBL) over the southeastern tropical Pacific. In particular, components of the VOCALS field campaign were designed to better characterize the dominant forms of mesoscale cellular convection (MCC), which in the southeastern tropical Pacific include closed cell and open cell structures, the latter with broken cloud and lower albedo. Pockets of open cells (POC) usually form within overcast closed MCC [Bretherton et al. 2004; Stevens et al. 2005; Comstock et al. 2007; Wood et al. 2008]. The transition from closed to open cells represents a shift from a system driven primarily by cloud-top longwave cooling to a more cumuliform structure in which lifting is in part forced at the surface by localized cold pools formed by the evaporation of drizzle [Wang and Feingold 2009; Feingold et al. 2010].

The intensive observational phase of VOCALS-REx took place during October and November 2008 and involved five aircraft, two ships and several ground sites [Wood et al. 2010; Wood et al. 2010a]. Satellite imagery of the 27/28 October 2008 POC event (Fig. 1a Sidebar) shows the formation of a POC aligned roughly NW-SE within overcast stratocumulus clouds early in the morning of 27 Oct. Ship radar observations (Fig 1b Sidebar) reveal locally intense drizzle cells surrounded by drizzle-free regions. The aircraft observations on the NE side sampled during the evening of 27 Oct and early morning of 28 Oct reveal marked transitions in drizzle structure, and in cloud and aerosol microphysical properties across the boundary [Wood et al. 2010]. Ship radar observations in the overcast region to the SW of the POC revealed the presence of more diffuse drizzling cells (Fig 1c Sidebar), that have peak rain rates less than the echoes observed within the POC. Subsequently, the POC evolved by growing in width and advecting to the NW with the synoptic flow. The VOCALS-REx dataset, along with complementary elements of the YOTC project (see companion article M11), provide promising avenues for improving our basic understanding of these processes, including capturing their bulk effects in our global weather and climate models.

7 Summary

The discussion above highlights the diverse and impactful nature of the weather and climate associated with the WCRP-WWRP/THORPEX YOTC period of interest. Notable is the wide range of scale interactions involving tropical convection, particularly in terms of how the influence of ENSO cascades across a number of time scales and phenomena including significant impacts on most of the monsoon circulations discussed, the nature of the intraseasonal variability, the structure and intensity of easterly waves, as well as the spatial modulation of extreme events such as tropical cyclones and atmospheric rivers. Significant highlights apart from the cool to warm transition in ENSO, are the severe drought monsoon for India in 2009 and the near record setting N. American monsoon in 2008. There was a fantastic tropical wave event in 2008 that impacted variability from the Indian to the Pacific/America sectors and extreme events in both the western and eastern hemisphere, and other examples of convectively-coupled wave-wave interactions. There were high impact rainfall events in Africa that derived from tropical sources (i.e. easterly waves) in both 2008 and 2009 and a number of cases that arose from the influence of the extratropics. The tropical

1 cyclone activity during YOTC, while being exceptionally quiet relative to the last 30 years,
2 exhibited numerous highlights, including Ike – one of the largest storm ever recorded in aerial
3 size in the Atlantic, Nargis - that led to disastrous consequences in Myanmar, three hurricanes
4 making landfall onto Mexico from the Pacific in 2008, the 1.8 m of rainfall over the Philippines
5 from slow moving Typhoon Parma, Rick – the second strongest hurricane on record in the
6 Pacific, high latitude hurricane Grace tracking across the United Kingdom, and a highly
7 unusual South Atlantic storm named Anita. Moreover, the impact of ETs on the midlatitude
8 flow during the entire YOTC period exhibits substantial variability both in terms of the
9 excitation of Rossby wavetrains and the predictive skill of this process. The objectives of
10 YOTC are to highlight these types of features and phenomena and promote their interrogation
11 via theory, observations and models so that improved understanding and predictions can be
12 afforded.

13 With the backing of the World Climate Research Program and World Weather Research
14 Program/THORPEX, the YOTC research program is developing a suite of state-of-the-art data
15 sets to examine the aforementioned weather and climate highlights in more detail. These
16 include high-resolution atmospheric analyses from ECMWF, NCEP and NASA and a number of
17 satellite data products including a multi-sensor co-located dataset based on the Earth
18 Observing System's A-Train. Moreover, the YOTC period occurred in conjunction with the T-
19 PARC and VOCALS field programs as well as a multitude of activities associated with the Asian
20 Monsoon Year (AMY), all of which allow additional resources and focus to be brought to bear
21 on interrelated tropical convection issues. By leveraging these activities and resources, the
22 YOTC Implementation Plan sets a course to develop a number of programmatic research
23 activities, model studies and intercomparisons. One particular focus is on using models in
24 hindcast mode to explore their sensitivities and shortcomings in conjunction with the above
25 observation resources to drive at improvements in our forecast capabilities from short-term
26 to seasonal prediction. This program and its focus provide an initial framework to develop the
27 techniques and know-how to approach the next generation of high-resolution models [e.g.,
28 global cloud-system resolving models (CSRMs), multi-scale modeling framework (MMF),
29 regional and adaptive grid systems] that at present tax our abilities to fully exploit all our
30 resources – both in terms of technical (e.g. network and analysis bandwidth) and scientific
31 (multi-scale interactions, multi-sensor constraints/evaluation) challenges. In this regard,
32 YOTC provides an excellent and rich activity through which to entrain and train the next
33 generation of weather, climate and Earth scientists through graduate and postdoctoral
34 research programs along with YOTC related meetings and symposia⁶. This new generation
35 will be ideally situated to capitalize on the new capabilities that have and are being put into
36 place, including the interdisciplinary education and landscape being established to tackle the
37 pressing environmental and societally impactful challenges associated with tropical
38 convection. Focused period field programs, with YOTC representing a global virtual field
39 program, represent key resources for the training scientists for many years to decades after
40 their initial data acquisition (e.g. www.ametsoc.org/sloan/gate/). For additional motivation,
41 scientific underpinnings and hypotheses associated with YOTC, see M11.

⁶ Past activities include YOTC-sponsored sessions at six American Geophysical Union meetings, a session at an American Meteorological Society Annual Meeting, 1st YOTC Science Symposia and a workshop on intraseasonal variability and the monsoon (see www.ucar.edu/yotc/meetings.html).

1
2
3
4
5
6
7
8
9
10
11
12
13
14
15
16
17
18
19
20

Acknowledgements

We would like to express our gratitude to the World Climate Research Program, the World Weather Research Program and The Observing system Research and Prediction Experiment (THORPEX) for their joint support of the YOTC program. This research has been supported by the National Science Foundation, Mesoscale Dynamic Meteorology Program, under Grant No. ATM-0639461 and the National Oceanic and Atmospheric Administration, Office of Global Programs, under Grant No. NA07OAR4310263. The European Centre for Medium-Range Weather Forecasts is acknowledged for providing the special ECMWF YOTC data set. We thank Paul Ciesielski and Andy Newman for assistance in the preparation of figures. The Cloudsat and TRMM data were visualized with the Giovanni online data system, developed and maintained by the NASA GES DISC. The Meteosat image was downloaded from the webpage of the Dundee Satellite Receiving Station. We are grateful to the ECMWF for providing access to the YOTC analysis and forecast products, and to the French IRD and the National Weather Services of Benin, Guinea, and Ghana for providing rainfall data for February 2009. BNG thanks Neena Mani Joseph and Suhas E for help in creating the Indian Monsoon figures. YLS was supported by NOAA's Climate Program Office under grant NA06OAR43100. DJG was supported by NOAA Climate Program Office Grant No. NA08OAR4310705.

1 **References**

- 2 Ajayamohan, R. S., S. A. Rao, and T. Yamagata, 2008: Influence of Indian Ocean Dipole on
3 Poleward Propagation of Boreal Summer Intraseasonal Oscillations. *Journal of Climate*,
4 **21**, 5437-5454.
- 5 Ajayamohan, R. S., S. A. Rao, J.-J. Luo, and T. Yamagata, 2009: Influence of Indian Ocean Dipole
6 on boreal summer intraseasonal oscillations in a CGCM. *Journal of Geophysical Research*,
7 **114**, D06119, doi:10.1029/2008JD011096.
- 8 Ambaum, M. H. P., B. J. Hoskins, and D. B. Stephenson, 2001: Arctic oscillation or North Atlantic
9 oscillation? *Journal of Climate*, **14**, 3495-3507.
- 10 Anwender, D., P. A. Harr, and S. C. Jones, 2008: Predictability associated with the downstream
11 impacts of the extratropical transition of tropical cyclones: Case studies. *Monthly*
12 *Weather Review*, **136**, 3226-3247.
- 13 Barlow, M., 2011: Africa and West Asia. *Intraseasonal Variability of the Atmosphere-Ocean*
14 *Climate System, 2nd Edition*, W. K. M. Lau, and D. E. Waliser, Eds., Springer, Heidelberg,
15 Germany.
- 16 Black, E., J. Slingo, and K. R. Sperber, 2003: An observational study of the relationship between
17 excessively strong short rains in coastal East Africa and Indian Ocean SST. *Monthly*
18 *Weather Review*, **131**, 74-94.
- 19 Bond, N. A., and G. A. Vecchi, 2003: The influence of the Madden-Julian oscillation on
20 precipitation in Oregon and Washington. *Weather and Forecasting*, **18**, 600-613.
- 21 Bretherton, C. S., T. Uttal, C. W. Fairall, S. E. Yuter, R. A. Weller, D. Baumgardner, K. Comstock,
22 R. Wood, and G. B. Raga, 2004: The EPIC 2001 stratocumulus study. *Bulletin of the*
23 *American Meteorological Society*, **85**, 967-+.
- 24 Carton, J., and B. Huang, 1994: Warm events in the tropical Atlantic. *Journal of Physical*
25 *Oceanography*, **24**, 888-903.
- 26 Carvalho, L. M. V., C. Jones, A. E. Silva, B. Liebmann, and P. L. Silva Dias, 2011: - The South
27 American Monsoon System and the 1970s climate transition, - **31**, - 1256.
- 28 Castro, C. L., T. B. McKee, and R. A. Pielke, 2001: The relationship of the North American
29 monsoon to tropical and North Pacific sea surface temperatures as revealed by
30 observational analyses. *J. Climate*, **14**, 4449-4473.
- 31 Cavazos, T., and S. Hastenrath, 1990: Convection and rainfall over Mexico and their
32 modulation by the southern oscillation. *International Journal of Climatology*, **10**, 377-
33 386.
- 34 Cerne, B., and C. S. Vera, 2010.: Influence of the intraseasonal variability on heat waves in
35 subtropical South America. *Climate Dynamics*, DOI: 10.1007/s00382-00010-00812-
36 00384.
- 37 Comstock, K. K., S. E. Yuter, R. Wood, and C. S. Bretherton, 2007: The three-dimensional
38 structure and kinematics of drizzling stratocumulus. *Monthly Weather Review*, **135**,
39 3767-3784.
- 40 Deser, C., 2000: On the teleconnectivity of the "Arctic Oscillation". *Geophysical Research*
41 *Letters*, **27**, 779-782.
- 42 Drosowsky, W., 1996: Variability of the Australian summer monsoon at Darwin: 1957-1992.
43 *Journal of Climate*, **9**, 85-96.
- 44 Enfield, D. B., and D. A. Mayer, 1997: Tropical Atlantic sea surface temperature variability and
45 its relation to El Niño Southern Oscillation. *Journal of Geophysical Research-Oceans*, **102**,
46 929-945.

- 1 Englehart, P. J., and A. V. Douglas, 2001: The role of eastern North Pacific tropical storms in the
2 rainfall climatology of western Mexico. *International Journal of Climatology*, **21**, 1357-
3 1370.
- 4 Feingold, G., I. Koren, H. Wang, H. Xue, and W. A. Brewer, 2010: Precipitation-generated
5 oscillations in open cellular cloud fields. *Nature*, **466**, 849–852, doi:10.1038.
- 6 Fink, A. H., J. M. Schrage, and S. Kothaus, 2010: On the Potential Causes of the Nonstationary
7 Correlations between West African Precipitation and Atlantic Hurricane Activity.
8 *Journal of climate*, **In Press**.
- 9 Gadgil, S., 1981: Fluid-Dynamics of the Monsoon. *Proceedings of the Indian Academy of*
10 *Sciences-Engineering Sciences*, **4**, 295-&.
- 11 Giannini, A., M. A. Cane, and Y. Kushnir, 2001: Interdecadal changes in the ENSO
12 teleconnection to the Caribbean region and the North Atlantic oscillation. *Journal of*
13 *Climate*, **14**, 2867-2879.
- 14 Gochis, D. J., L. Brito-Castillo, and W. J. Shuttleworth, 2007: Correlations between sea-surface
15 temperatures and warm season streamflow in northwest Mexico. *International Journal*
16 *of Climatology*, **27**, 883-901.
- 17 Gochis, D. J., S. W. Nesbitt, W. Yu, and S. F. Williams, 2009: Comparison of gauge-corrected
18 versus non-gauge corrected satellite-based quantitative precipitation estimates during
19 the 2004 NAME enhanced observing period. *Atmosfera*, **22**, 69-98.
- 20 Goswami, B. N., 2011: South Asian Summer Monsoon. *Intraseasonal Variability of the*
21 *Atmosphere-Ocean Climate System, 2nd Edition*, W. K. M. Lau, and D. E. Waliser, Eds.,
22 Springer, Heidelberg, Germany.
- 23 Grimm, A. M., and M. Zilli, 2009: Interannual variability and seasonal evolution of summer
24 monsoon in South America. *Journal of Climate*, , **22**, 2257–2275.
- 25 Grimm, A. M., 2010: Interannual climate variability in South America: impacts on seasonal
26 precipitation, extreme events and possible effects of climate change. . *Stochastic*
27 *Environmental Research and Risk Assessment*, DOI: 10.1007/s00477-00010-00420-
28 00471.
- 29 Guan, B., N. P. Molotch, D. E. Waliser, E. J. Fetzer, P. J. Neiman, and Geophys. Res. Lett., 2010:
30 Extreme snowfall events linked to atmospheric rivers and surface air temperature via
31 satellite measurements. *Geophys. Res. Lett.*, doi:10.1029/2010GL044696.
- 32 Hagos, S., and K. Cook, 2007: Dynamics of the West African monsoon jump. *Journal of Climate*,
33 **20**, 5264–5284.
- 34 Harr, P. A., D. Anwender, and S. C. Jones, 2008: Predictability associated with the downstream
35 impacts of the extratropical transition of tropical cyclones: Methodology and a case
36 study of Typhoon Nabi (2005). *Monthly Weather Review*, **136**, 3205-3225.
- 37 Harr, P. A., and J. M. Dea, 2009: Downstream Development Associated with the Extratropical
38 Transition of Tropical Cyclones over the Western North Pacific. *Monthly Weather*
39 *Review*, **137**, 1295-1319.
- 40 Hastenrath, S., 1987: On the Prediction of India Monsoon Rainfall Anomalies. *Journal of*
41 *Climate and Applied Meteorology*, **26**, 847-857.
- 42 Hastenrath, S., and L. Greischar, 2001: The North Atlantic oscillation in the NCEP-NCAR
43 reanalysis. *Journal of Climate*, **14**, 2404-2413.
- 44 Hendon, H. H., C. D. Zhang, and J. D. Glick, 1999: Interannual variation of the Madden-Julian
45 oscillation during austral summer. *Journal of Climate*, **12**, 2538-2550.
- 46 Hendon, H. H., M. C. Wheeler, and C. D. Zhang, 2007: Seasonal dependence of the MJO-ENSO
47 relationship. *Journal of Climate*, **20**, 531-543.

- 1 Higgins, R. W., K. C. Mo, and Y. Yao, 1998: Interannual variability of the US summer
2 precipitation regime with emphasis on the southwestern monsoon. *Journal of Climate*,
3 **11**, 2582-2606.
- 4 Higgins, R. W., W. Shi, and C. Hain, 2004: Relationships between Gulf of California moisture
5 surges and precipitation in the southwestern United States. *Journal of Climate*, **17**,
6 2983-2997.
- 7 Horel, J. D., and J. M. Wallace, 1981: Planetary-Scale Atmospheric Phenomena Associated with
8 the Southern Oscillation. *Monthly Weather Review*, **109**, 813-829.
- 9 ———, 1982: Planetary-Scale Atmospheric Phenomena Associated with the Southern
10 Oscillation - Reply. *Monthly Weather Review*, **110**, 1497-1497.
- 11 Hsieh, J. S., and K. H. Cook, 2005: Generation of African easterly wave disturbances:
12 Relationship to the African easterly jet. *Monthly Weather Review*, **133**, 1311-1327.
- 13 ———, 2007: A study of the energetics of African easterly waves using a regional climate model.
14 *Journal of the Atmospheric Sciences*, **64**, 421-440.
- 15 Hsu, P. C., C. H. Tsou, H. H. Hsu, and J. H. Chen, 2009: Eddy Energy along the Tropical Storm
16 Track in Association with ENSO. *Journal of the Meteorological Society of Japan*, **87**, 687-
17 704.
- 18 Huffman, G. J., R. F. Adler, D. T. Bolvin, G. Gu, E. J. Nelkin, K. P. Bowman, Y. Hong, E. F. Stocker,
19 and D. B. Wolff, 2007: The TRMM Multisatellite Precipitation Analysis (TMPA): Quasi-
20 Global, Multiyear, Combined-Sensor Precipitation Estimates at Fine Scales. *Journal of*
21 *Hydrometeorology*, **8**, 38-55.
- 22 Hurrell, J. W., 1996: Influence of variations in extratropical wintertime teleconnections on
23 Northern Hemisphere temperature. *Geophysical Research Letters*, **23**, 665-668.
- 24 Janicot, S., and Coauthors, 2008: Large-scale overview of the summer monsoon over West
25 Africa during the AMMA field experiment in 2006. *Annales Geophysicae*, **26**, 2569-2595.
- 26 Janiga, M. A., 2010: Easterly wave structural evolution over West Africa and the East Atlantic.
27 *29th Conference on Hurricanes and Tropical Meteorology*, Tuscon, AZ.
- 28 Jones, C., 2000: Occurrence of extreme precipitation events in California and relationships
29 with the Madden-Julian oscillation. *Journal of Climate*, **13**, 3576-3587.
- 30 Jones, S. C., and Coauthors, 2003: The extratropical transition of tropical cyclones: Forecast
31 challenges, current understanding, and future directions. *Weather and Forecasting*, **18**,
32 1052-1092.
- 33 Joseph, S., A. K. Sahai, and B. N. Goswami, 2009: Boreal summer intraseasonal oscillations and
34 seasonal Indian monsoon prediction in DEMETER coupled models. *Climate Dynamics*,
35 **DOI 10.1007/s00382-009-0635-3**.
- 36 Kessler, W. S., 2001: EOF representations of the Madden-Julian oscillation and its connection
37 with ENSO. *Journal of Climate*, **14**, 3055-3061.
- 38 Kiladis, G. N., C. D. Thorncroft, and N. M. J. Hall, 2006: Three-dimensional structure and
39 dynamics of African easterly waves. Part I: Observations. *Journal of the Atmospheric*
40 *Sciences*, **63**, 2212-2230.
- 41 Kiladis, G. N., M. C. Wheeler, P. T. Haertel, K. H. Straub, and P. E. Roundy, 2009: Convectively
42 coupled equatorial waves. *Reviews of Geophysics*, **47**.
- 43 Knippertz, P., and J. E. Martin, 2005: Tropical plumes and extreme precipitation in subtropical
44 and tropical West Africa. *Quarterly Journal of the Royal Meteorological Society*, **131**,
45 2337-2365.
- 46 Knippertz, P., 2007: Tropical-extratropical interactions related to upper-level troughs at low
47 latitudes. *Dynamics of Atmospheres and Oceans*, **43**, 36-62.

- 1 Knippertz, P., and A. H. Fink, 2008: Dry-season precipitation in tropical West Africa and its
2 relation to forcing from the extratropics. *Monthly Weather Review*, **136**, 3579-3596.
- 3 ———, 2009: Prediction of Dry-Season Precipitation in Tropical West Africa and Its Relation to
4 Forcing from the Extratropics. *Weather and Forecasting*, **24**, 1064-1084.
- 5 Kumar, A., and M. P. Hoerling, 1998: Annual cycle of Pacific North American seasonal
6 predictability associated with different phases of ENSO. *Journal of Climate*, **11**, 3295-
7 3308.
- 8 L'Heureux, M. L., and R. W. Higgins, 2008: Boreal winter links between the Madden-Julian
9 oscillation and the Arctic oscillation. *Journal of Climate*, **21**, 3040-3050.
- 10 Lau, K. M., and H. Lim, 1982: Thermally Driven Motions in a Equatorial Beta-Plane - Hadley
11 and Walker Circulations During the Winter Monsoon. *Monthly Weather Review*, **110**,
12 336-353.
- 13 Lau, N. C., and M. J. Nath, 2006: ENSO Modulation of the Interannual and Intraseasonal
14 Variability of the East Asian Monsoon—A Model Study. *Journal of Climate*, **19**.
- 15 Lau, W. K. M., 2005: ENSO Connections. *Intraseasonal Variability of the Atmosphere-Ocean
16 Climate System*, W. K. M. Lau, and D. E. Waliser, Eds., Springer, Heidelberg, Germany.
- 17 Lau, W. K. M., and D. E. Waliser, Eds., 2011: *Intraseasonal Variability of the Atmosphere-Ocean
18 Climate System, 2nd Edition*. Springer, Heidelberg, Germany, TBD pp.
- 19 Leroux, S., and N. M. J. Hall, 2009: On the Relationship between African Easterly Waves and the
20 African Easterly Jet. *Journal of the Atmospheric Sciences*, **66**, 2303-2316.
- 21 Leroux, S., N. M. J. Hall, and G. N. Kiladis, 2010: A climatological study of transient-mean-flow
22 interactions over West Africa. *Quarterly Journal of the Royal Meteorological Society*, **136**,
23 397-410.
- 24 Leroux, S., N. M. J. Hall, and G. N. Kiladis, 2011: Intermittent African Easterly Wave activity in a
25 dry atmospheric model: influence of the extratropics. *Journal of Climate*, **In Press**.
- 26 Liebmann, B., and J. A. Marengo, 2001: Interannual variability of the rainy season and rainfall
27 in the Brazilian Amazon basin. *Journal of Climate*, **14**, 4308-4318.
- 28 Liebmann, B., G. N. Kiladis, C. S. Vera, A. C. Saulo, and L. M. V. Carvalho, 2004: Subseasonal
29 variations of rainfall in South America in the vicinity of the low-level jet east of the
30 Andes and comparison to those in the South Atlantic convergence zone. *Journal of
31 Climate*, **17**, 3829-3842.
- 32 Liebmann, B., S. J. Camargo, A. Seth, J. A. Marengo, L. M. V. Carvalho, D. Allured, R. Fu, and C. S.
33 Vera, 2007: Onset and end of the rainy season in South America in observations and the
34 ECHAM 4.5 atmospheric general circulation model. *Journal of Climate*, **20**, 2037-2050.
- 35 Liebmann, B., I. Blade, N. A. Bond, D. Gochis, D. Allured, and G. T. Bates, 2008: Characteristics
36 of north American summertime rainfall with emphasis on the monsoon. *Journal of
37 Climate*, **21**, 1277-1294.
- 38 Madden, R. A., and P. R. Julian, 1971: Detection of a 40-50 Day Oscillation in Zonal Wind in
39 Tropical Pacific. *Journal of the Atmospheric Sciences*, **28**, 702-&.
- 40 Magana, V., and M. Yanai, 1995: Mixed Rossby-Gravity Waves Triggered by Lateral Forcing.
41 *Journal of the Atmospheric Sciences*, **52**, 1473-1486.
- 42 Marengo, J., and Coauthors, 2010: New developments on the functioning, characteristics and
43 variability of the South American Monsoon System,. *Int. J. Climatology, In press*.
- 44 Marengo, J. A., J. Tomasella, W R. Soares, L. M. Alves, and C. A. Nobre, 2011a: Extreme climatic
45 events in the Amazon basin: Climatological and hydrological context of recent floods, .
46 *Theoretical and Applied Climatology*, DOI 10.1007/s00704-011-0465-1.

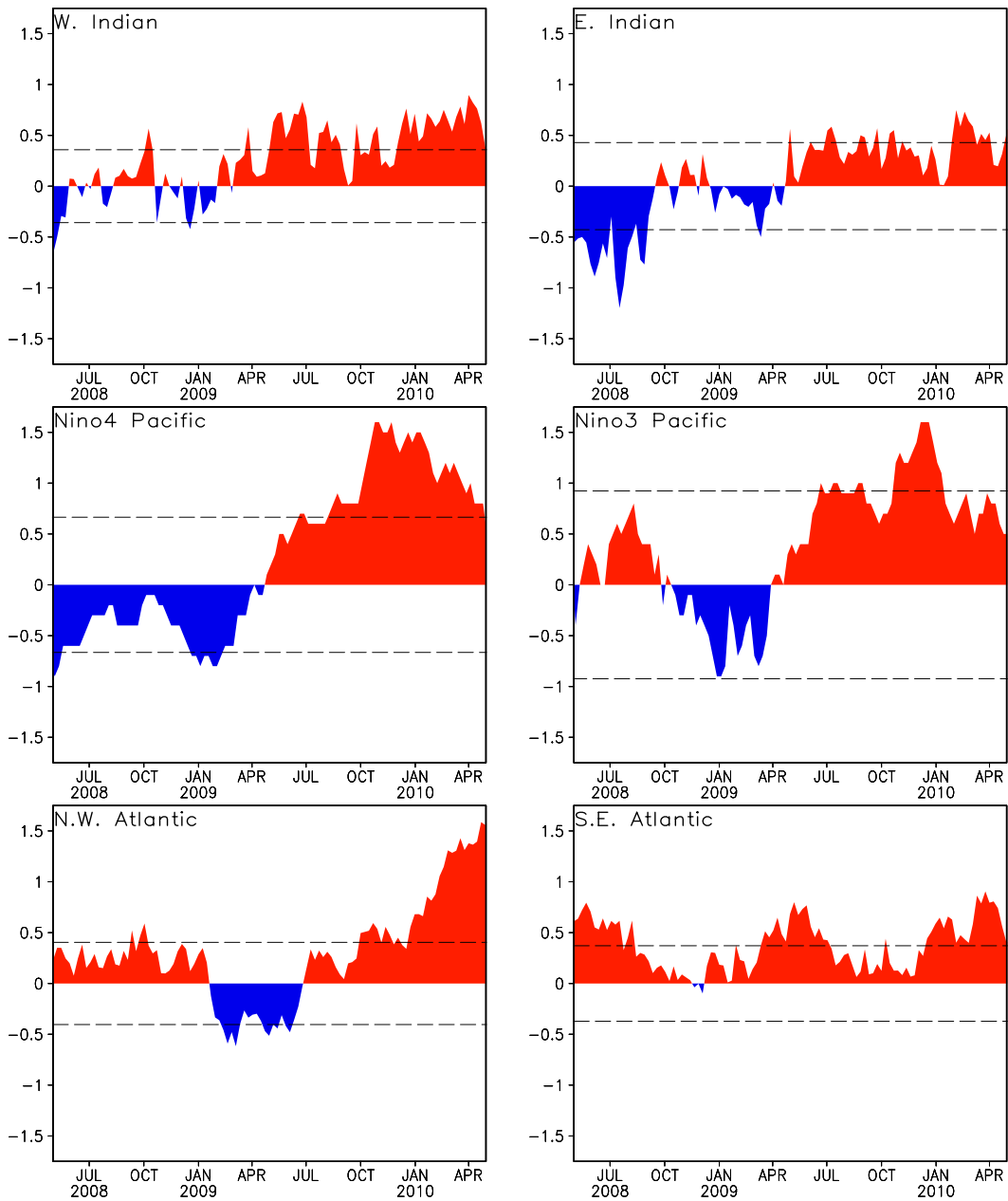
- 1 Marengo, J. A., J. Tomasella, L. M. Alves, W. R. Soares, and D. A. Rodriguez, 2011b: The drought
2 of 2010 in the context of historical droughts in the Amazon region. *Geophysical Research*
3 *Letters*, **38**, L12703, doi:10.1029/2011GL047436.
- 4 Maue, R. N., 2009: Northern Hemisphere tropical cyclone activity. *Geophysical Research*
5 *Letters*, **36**, doi:10.1029/2008GL035946.
- 6 —, 2011: Recent historically low global tropical cyclone activity. *Geophysical Research*
7 *Letters*, **38**, doi:10.1029/2011GL047711.
- 8 Meier, F., and P. Knippertz, 2009: Dynamics and Predictability of a Heavy Dry-Season
9 Precipitation Event over West Africa-Sensitivity Experiments with a Global Model.
10 *Monthly Weather Review*, **137**, 189-206.
- 11 Mekonnen, A., C. D. Thorncroft, and A. R. Aiyyer, 2006: Analysis of convection and its
12 association with African easterly waves. *Journal of Climate*, **19**, 5405-5421.
- 13 Mekonnen, A., C. D. Thorncroft, A. R. Aiyyer, and G. N. Kiladis, 2008: Convectively Coupled
14 Kelvin Waves over Tropical Africa during the Boreal Summer: Structure and Variability.
15 *Journal of Climate*, **21**, 6649-6667.
- 16 Mo, K. C., and R. W. Higgins, 1998a: Tropical influences on California precipitation. *Journal of*
17 *Climate*, **11**, 412-430.
- 18 —, 1998b: Tropical convection and precipitation regimes in the western United States.
19 *Journal of Climate*, **11**, 2404-2423.
- 20 Moncrieff, M. W., M. Shapiro, J. Slingo, and F. Molteni, 2007: Collaborative research at the
21 intersection of weather and climate. *WMO Bulletin*, **56**, 204-211.
- 22 Murakami, T., 1975: Temporal Variation of Monsoon Circulation. *Bulletin of the American*
23 *Meteorological Society*, **56**, 309-309.
- 24 Neena, J. M., E. Suhas, and i. B. N. Goswam, 2011: Leading role of internal dynamics in the 2009
25 Indian Summer Monsoon drought. *Journal of Geophysical Research*, **116D**.
- 26 Neiman, P. J., F. M. Ralph, G. A. Wick, Y. H. Kuo, T. K. Wee, Z. Z. Ma, G. H. Taylor, and M. D.
27 Dettinger, 2008a: Diagnosis of an Intense Atmospheric River Impacting the Pacific
28 Northwest: Storm Summary and Offshore Vertical Structure Observed with COSMIC
29 Satellite Retrievals. *Monthly Weather Review*, **136**, 4398-4420.
- 30 Neiman, P. J., F. M. Ralph, G. A. Wick, J. D. Lundquist, and M. D. Dettinger, 2008b:
31 Meteorological characteristics and overland precipitation impacts of atmospheric rivers
32 affecting the West Coast of North America based on eight years of SSM/I satellite
33 observations. *Journal of Hydrometeorology*, **9**, 22-47.
- 34 Newman, M., and P. D. Sardeshmukh, 1998: The impact of the annual cycle on the North Pacific
35 North American response to remote low-frequency forcing. *Journal of the Atmospheric*
36 *Sciences*, **55**, 1336-1353.
- 37 Nguyen, T. T. H., and J. P. Duvel, 2008: Synoptic wave perturbations and convective systems
38 over equatorial Africa. *Journal of Climate*, **21**, 6372-6388.
- 39 Nicholls, N., J. L. McBride, and R. J. Ormerod, 1982: On predicting the onset of the Australian
40 wet season at Darwin. *Monthly Weather Review*, **110**, 14-17.
- 41 Nicholson, S. E., and P. J. Webster, 2007: A physical basis for the interannual variability of
42 rainfall in the Sahel. *Quarterly Journal of the Royal Meteorological Society*, **133**, 2065-
43 2084.
- 44 Nieto-Ferreira, R., and T. M. Rickenbach, 2011: - Regionality of monsoon onset in South
45 America: a three-stage conceptual model, - **31**, - 1321.

- 1 Nitta, T., and Y. Takayabu, 1985: Global Analysis of the lower tropospheric disturbances in the
2 tropics during the northern summer of the FGGE Year Part II: Regional Characteristics
3 of the Disturbances. *PAGEOPH*, **123**, 272-292.
- 4 Nogues-Paegle, J., and K. C. Mo, 1997: Alternating wet and dry conditions over South America
5 during summer. *Monthly Weather Review*, **125**, 279-291.
- 6 Okumura, Y., and S. P. Xie, 2004: Interaction of the Atlantic equatorial cold tongue and the
7 African monsoon. *Journal of Climate*, **17**, 3589-3602.
- 8 Ostermeier, G. M., and J. M. Wallace, 2003: Trends in the North Atlantic Oscillation-Northern
9 Hemisphere annular mode during the twentieth century. *Journal of Climate*, **16**, 336-
10 341.
- 11 Pohl, B., N. Fauchereau, C. J. C. Reason, and M. Rouault, 2010: Relationships between the
12 Antarctic Oscillation, the Madden - Julian Oscillation, and ENSO, and Consequences for
13 Rainfall Analysis. *Journal of Climate*, **23**, 238-254.
- 14 Pope, M., C. Jakob, and M. J. Reeder, 2009: Regimes of the North Australian Wet Season. *Journal*
15 *of Climate*, **22**, 6699-6715.
- 16 Ralph, F. M., P. J. Neiman, and G. A. Wick, 2004: Satellite and CALJET aircraft observations of
17 atmospheric rivers over the eastern north pacific ocean during the winter of 1997/98.
18 *Monthly Weather Review*, **132**, 1721-1745.
- 19 Ralph, F. M., P. J. Neiman, G. A. Wick, S. I. Gutman, M. D. Dettinger, D. R. Cayan, and A. B. White,
20 2006: Flooding on California's Russian River: Role of atmospheric rivers. *Geophysical*
21 *Research Letters*, **33**.
- 22 Ralph, F. M., P. J. Neiman, G. N. Kiladis, K. Weickmann, and D. W. Reynolds, 2011: A Multiscale
23 Observational Case Study of a Pacific Atmospheric River Exhibiting Tropical-
24 Extratropical Connections and a Mesoscale Frontal Wave. *Monthly Weather Review*, **139**,
25 1169-1189.
- 26 Ramage, C. S., 1971: *Monsoon Meteorology*. Vol. 15, Academic Press, 296 pp.
- 27 Ramel, R., H. Gallée, and C. Messenger, 2006: On the northward shift of the West African
28 monsoon. *Climate Dynamics*, **26**, 429-440.
- 29 Rao, S. A., S. Masson, J.-J. Luo, S. K. Behera, and T. Yamagata, 2007: Termination of Indian
30 Ocean Dipole events in a coupled general circulation model. *Journal of Climate*, **20**,
31 **3018-3035**, doi:10.1175/JCLI4164.1.
- 32 Redelsperger, J. L., C. D. Thorncroft, A. Diedhiou, T. Lebel, D. J. Parker, and J. Polcher, 2006:
33 African monsoon multidisciplinary analysis - An international research project and field
34 campaign. *Bulletin of the American Meteorological Society*, **87**, 1739-+.
- 35 Reed, R., and E. Recker, 1971: Structure and Properties of Synoptic-Scale Wave Disturbances
36 in the Equatorial Western Pacific. *Journal of the Atmospheric Sciences*, **28**, 1117-1133
- 37 Reed, R., D. Norquist, and E. Recker, 1977: The structure and properties of African wave
38 disturbances as observed during Phase III of GATE. *Monthly Weather Review* **105**, 317-
39 333.
- 40 Renwick, J. A., and J. M. Wallace, 1996: Relationships between North Pacific wintertime
41 blocking, El Nino, and the PNA pattern. *Monthly Weather Review*, **124**, 2071-2076.
- 42 Rodwell, M. J., and B. J. Hoskins, 2001: Subtropical anticyclones and summer monsoons.
43 *Journal of Climate*, **14**, 3192-3211.
- 44 Roundy, P., 2011: Tropical-Extratropical Interactions. *Intraseasonal Variability of the*
45 *Atmosphere-Ocean Climate System, 2nd Edition*, W. K. M. Lau, and D. E. Waliser, Eds.,
46 Springer, Heidelberg, Germany, TBD.

- 1 Ryoo, J. M., D. Waliser, and E. Fetzer, 2011: Trajectory analysis on the origin of air mass and
2 moisture associated with Atmospheric Rivers over the west coast of the United States.
3 *Atmospheric Chemistry and Physics Discussions*, **11**, 11109-11142.
- 4 Saji, N. H., B. N. Goswami, P. N. Vinayachandran, and T. Yamagata, 1999: A dipole mode in the
5 tropical Indian Ocean. *Nature*, **401**, 360-363.
- 6 Salio, P., M. Nicolini, and E. J. Zipser, 2007: Mesoscale convective systems over Southeastern
7 South America and their relationship with the South American Low Level Jet. *Monthly*
8 *Weather Review*, **135**, 1290-1309.
- 9 Serra, Y., G. N. Kiladis, and M. F. Cronin, 2008: Horizontal and vertical structure of easterly
10 waves in the Pacific ITCZ. *Journal of the Atmospheric Sciences*, **65**, 1266-1284.
- 11 Serra, Y., 2009: Easterly wave activity and its modulation by the larger scales during the YOTC
12 time period of focus: May 2008-Oct 2009. *YOTC Session, American Geophysical Union*
13 *Annual Meeting, San Francisco, CA, Dec., 2009*.
- 14 Silva, V. B. S., and E. H. Berbery, 2006: Intense rainfall events affecting the La Plata basin. *J.*
15 *Hydrometeorology*, **7**.
- 16 Stevens, B., G. Vali, K. Comstock, R. Wood, M. C. van Zanten, P. H. Austin, C. S. Bretherton, and
17 D. H. Lenschow, 2005: Pockets of open cells and drizzle in marine stratocumulus.
18 *Bulletin of the American Meteorological Society*, **86**, 51-+.
- 19 Straub, K. H., and G. N. Kiladis, 2003: Extratropical forcing of convectively coupled Kelvin
20 waves during austral winter. *Journal of the Atmospheric Sciences*, **60**, 526-543.
- 21 Sultan, B., and S. Janicot, 2000: Abrupt shift of the ITCZ over West Africa and intra-seasonal
22 variability. *Geophysical Research Letters*, **27**, 3353-3356.
- 23 ———, 2003: The West African Monsoon Dynamics. Part II: The “Preonset” and “Onset” of the
24 Summer Monsoon. *Journal of Climate*, **16**, 3407-3427.
- 25 Takayabu, Y. N., 1994: Large-scale cloud disturbances associated with equatorial waves. Part
26 I: Spectral features of the cloud disturbances. *Journal of the Meteorological Society of*
27 *Japan*, **72**, 433-449.
- 28 Thompson, D. W. J., and J. M. Wallace, 1998: The Arctic Oscillation signature in the wintertime
29 geopotential height and temperature fields. *Geophysical Research Letters*, **25**, 1297-
30 1300.
- 31 ———, 2000: Annular modes in the extratropical circulation. Part I: Month-to-month variability.
32 *J. Climate*, **13**, 1000-1016.
- 33 Thorncroft, C., and K. Hodges, 2001: African Easterly Wave Variability and Its Relationship to
34 Atlantic Tropical Cyclone Activity. *J. Climate*, **14**, 116-1179.
- 35 Thorncroft, C. D., N. M. J. Hall, and G. N. Kiladis, 2008: Three-Dimensional Structure and
36 Dynamics of African Easterly Waves. Part III: Genesis. *Journal of the Atmospheric*
37 *Sciences*, **65**, 3596-3607.
- 38 Trenberth, K. E., D. P. Stepaniak, and J. M. Caron, 2000: The global monsoon as seen through
39 the divergent atmospheric circulation. *Journal of Climate*, **13**, 3969-3993.
- 40 Ventrice, M. J., C. D. Thorncroft, and M. A. Janiga, 2011: Atlantic tropical cyclogenesis: A three-
41 way interaction between an African easterly wave, diurnally varying convection, and a
42 convectively-coupled atmospheric Kelvin wave. *Monthly weather review*, **Submitted**.
- 43 Vera, C., and Coauthors, 2006: Toward a unified view of the American Monsoon Systems.
44 *Journal of Climate*, **19**, 4977-5000.
- 45 Waliser, D., Z. Zhang, K. M. Lau, and J. H. Kim, 2001: Interannual Sea Surface Temperature
46 Variability and the Predictability of Tropical Intraseasonal Variability. *Journal of the*
47 *Atmospheric Sciences*, **58**, 2595-2614.

- 1 Waliser, D. E., 2006: Intraseasonal Variability. *The Asian Monsoon*, B. Wang, Ed., Springer,
2 Heidelberg, Germany, 844
- 3 Waliser, D. E., and M. Moncrieff, 2008: The Year of Tropical Convection (YOTC) Science Plan: A
4 joint WCRP - WWRP/THORPEX International Initiative. .
- 5 Wallace, J. M., and D. S. Gutzler, 1981: Teleconnections in the Geopotential Height Field During
6 the Northern Hemisphere Winter. *Monthly Weather Review*, **109**, 784-812.
- 7 Wallace, J. M., 2000: North Atlantic Oscillation/annular mode: Two paradigms - one
8 phenomenon. *Quarterly Journal of the Royal Meteorological Society*, **126**, 791-805.
- 9 Wang, B., Ed., 2006: *The Asian Monsoon*. Springer, Heidelberg, Germany, 844 pp.
- 10 Wang, C. Z., S. K. Lee, and D. B. Enfield, 2008: Atlantic Warm Pool acting as a link between
11 Atlantic Multidecadal Oscillation and Atlantic tropical cyclone activity. *Geochemistry
12 Geophysics Geosystems*, **9**.
- 13 Wang, H. L., and G. Feingold, 2009: Modeling Mesoscale Cellular Structures and Drizzle in
14 Marine Stratocumulus. Part I: Impact of Drizzle on the Formation and Evolution of Open
15 Cells. *Journal of the Atmospheric Sciences*, **66**, 3237-3256.
- 16 Ward, M. N., 1998: Diagnosis and short-lead time prediction of summer rainfall in tropical
17 North Africa at interannual and multidecadal timescales. *Journal of Climate*, **11**, 3167-
18 3191.
- 19 Weickmann, K. M., G. R. Lussky, and J. E. Kutzbach, 1985: Intraseasonal (30-60 Day)
20 Fluctuations of Outgoing Longwave Radiation and 250-Mb Stream-Function During
21 Northern Winter. *Monthly Weather Review*, **113**, 941-961.
- 22 Wheeler, M., and G. N. Kiladis, 1999: Convectively coupled equatorial waves: Analysis of
23 clouds and temperature in the wavenumber-frequency domain. *Journal of the
24 Atmospheric Sciences*, **56**, 374-399.
- 25 Wheeler, M., and K. M. Weickmann, 2001: Real-time monitoring and prediction of modes of
26 coherent synoptic to intraseasonal tropical variability. *Mon. Wea. Rev.*, **129**, 2677-2694.
- 27 Wheeler, M. C., and H. H. Hendon, 2004: An all-season real-time multivariate MJO index:
28 Development of an index for monitoring and prediction. *Monthly Weather Review*, **132**,
29 1917-1932.
- 30 Wood, R., K. K. Comstock, C. S. Bretherton, C. Cornish, J. Tomlinson, D. R. Collins, and C. Fairall,
31 2008: Open cellular structure in marine stratocumulus sheets. *Journal of Geophysical
32 Research-Atmospheres*, **113**.
- 33 Wood, R., C. S. Bretherton, D. Leon, A. D. Clarke, P. Zuidema, G. Allen, and H. Coe, 2010: An
34 aircraft case study of the spatial transition from closed to open mesoscale cellular
35 convection. *Atmos. Chem. Phys., Disc.*, **10**, 17911-17980.
- 36 Wood, R., and Coauthors, 2010a: The VAMOS Ocean-Cloud-Atmosphere-Land Study Regional
37 Experiment (VOCALS-REx): Goals, platforms, and field operations. . *Atmos. Chem. Phys.
38 Discuss.*, **10**, 20769-20822.
- 39 Zhang, C. D., 2005: Madden-Julian Oscillation. *Reviews of Geophysics*, **43**.
- 40 Zhou, J. Y., and K. M. Lau, 1998: Does a monsoon climate exist over South America? *Journal of
41 Climate*, **11**, 1020-1040.
- 42 Zhu, Y., and R. E. Newell, 1994: Atmospheric rivers and bombs. *Geophysical Research Letters*,
43 **21**, 1999-2002.
- 44 —, 1998: A proposed algorithm for moisture fluxes from atmospheric rivers. *Monthly
45 Weather Review*, **126**, 725-735.

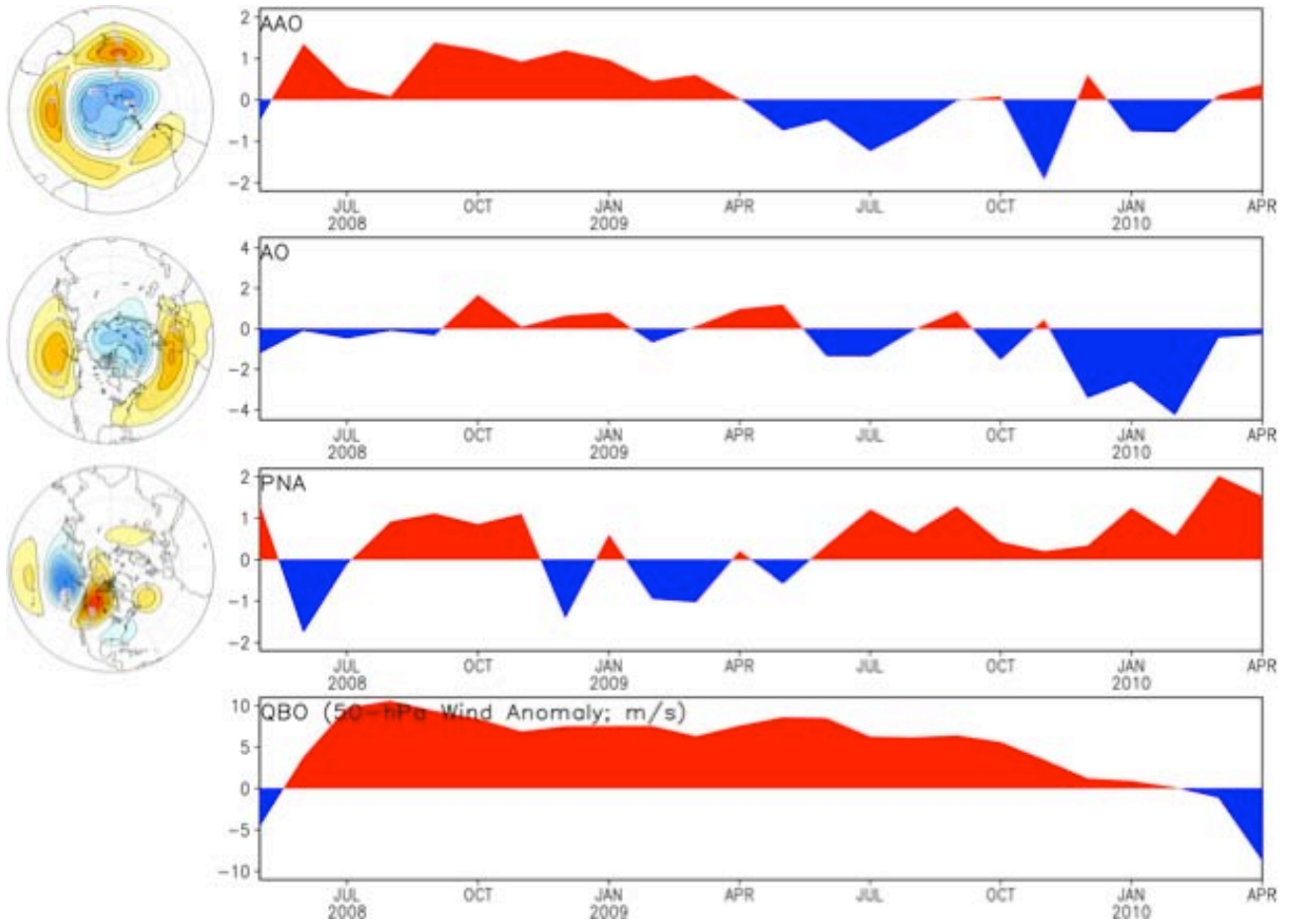
1 FIGURES



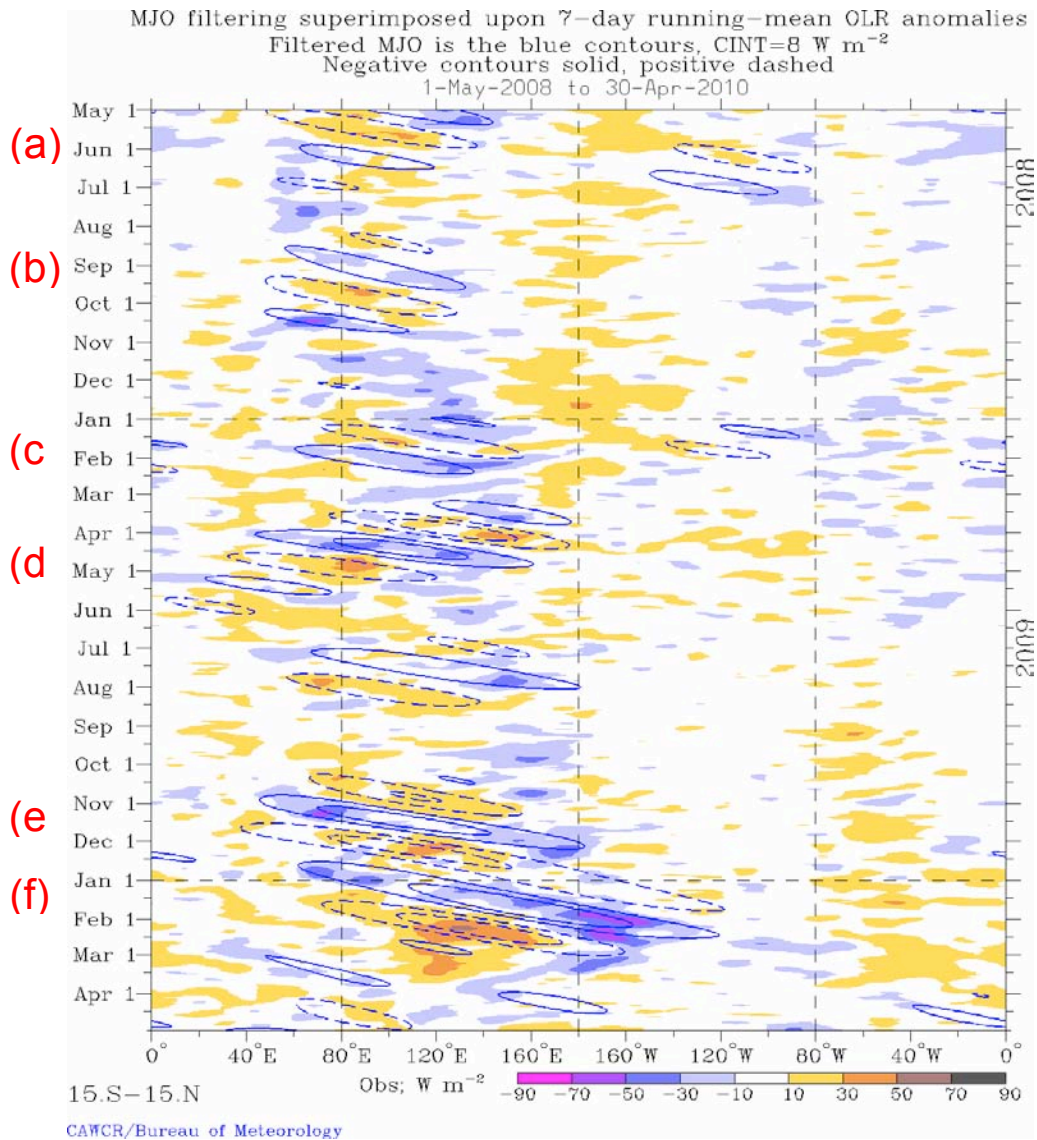
2

3 Figure 1. Tropical ocean SST anomalie (C) in terms of weekly values during the YOTC period. (upper left) West
 4 Indian Ocean (50°E - 70°E, 10°S - 10°N), (upper right) East Indian Ocean (90°E - 110°E, 10°S - 0°), (middle left)
 5 West Pacific Ocean (160°E - 150°W, 5°S - 5°N), (middle right) East Pacific Ocean (150°W - 90°W, 5°S - 5°N),
 6 (lower left) North Atlantic (55°W - 15°W, 5°N - 25°N), (lower right) South Atlantic (30°W - 10°E, 20°S - 0°).
 7 Notes: 1) The West (East) Pacific Ocean defined here are often referred to as Nino-4 and Nino-3; 2) subtracting
 8 the East from the West Indian Ocean time series gives the Indian Ocean Dipole (IOD) Mode Index [DMI, not
 9 shown, Saji et al. 1999]. Tropical Pacific time series are from www.cpc.noaa.gov/data/indices/, others time
 10 series are from ioc-goos-oopc.org/state_of_the_ocean/

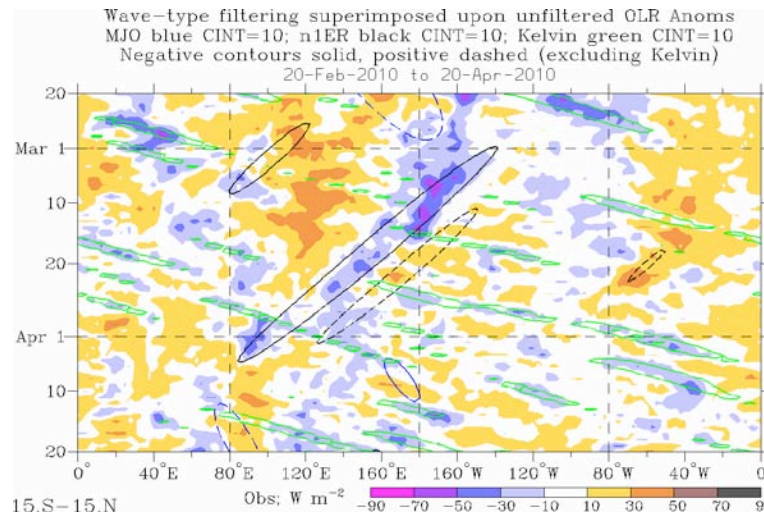
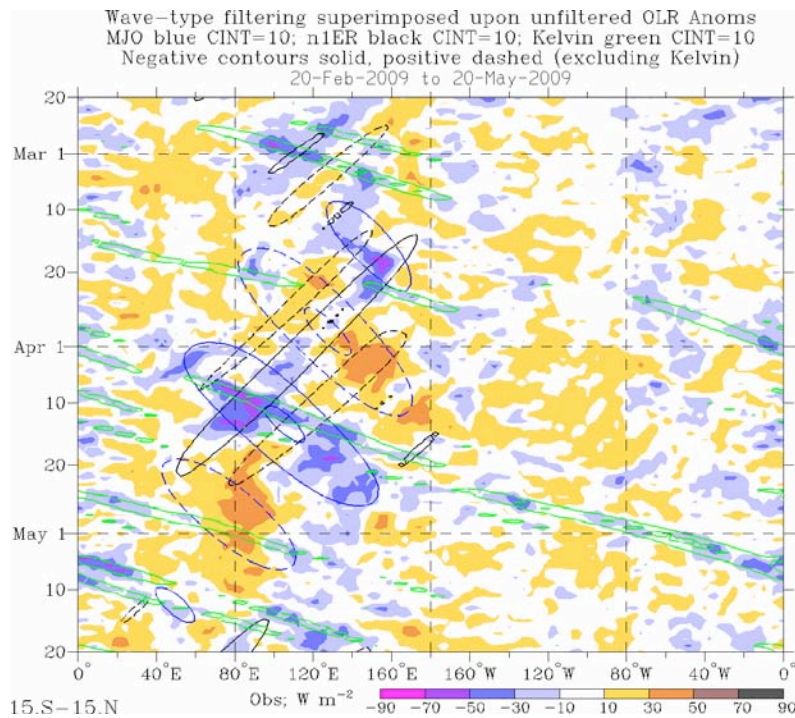
11



1
 2 Figure 2. Monthly time series of (from top to bottom) the Antarctic Oscillation (AAO),
 3 Arctic Oscillation (AO),
 4 Pacific North America (PNA), and the Quasi-Biennial Oscillation (QBO) for the YOTC period (unitless, except for
 5 QBO in m s^{-1}). To the left of the first three indices are the spatial patterns of the 500 hPa geopotential height
 6 anomaly patterns associated with each of the modes of variability; each contour represents 10 m. Indices are
 7 defined and the data obtained from the following two CPC/NCEP/NOAA web sites
 8 (www.cpc.noaa.gov/data/indices/,
 9 www.cpc.ncep.noaa.gov/products/precip/CWlink/daily_ao_index/teleconnections.shtml). The spatial patterns of the AAO, AO and PNA were
 10 obtained from <http://www.emc.ncep.noaa.gov/gmb/ssaha/>.



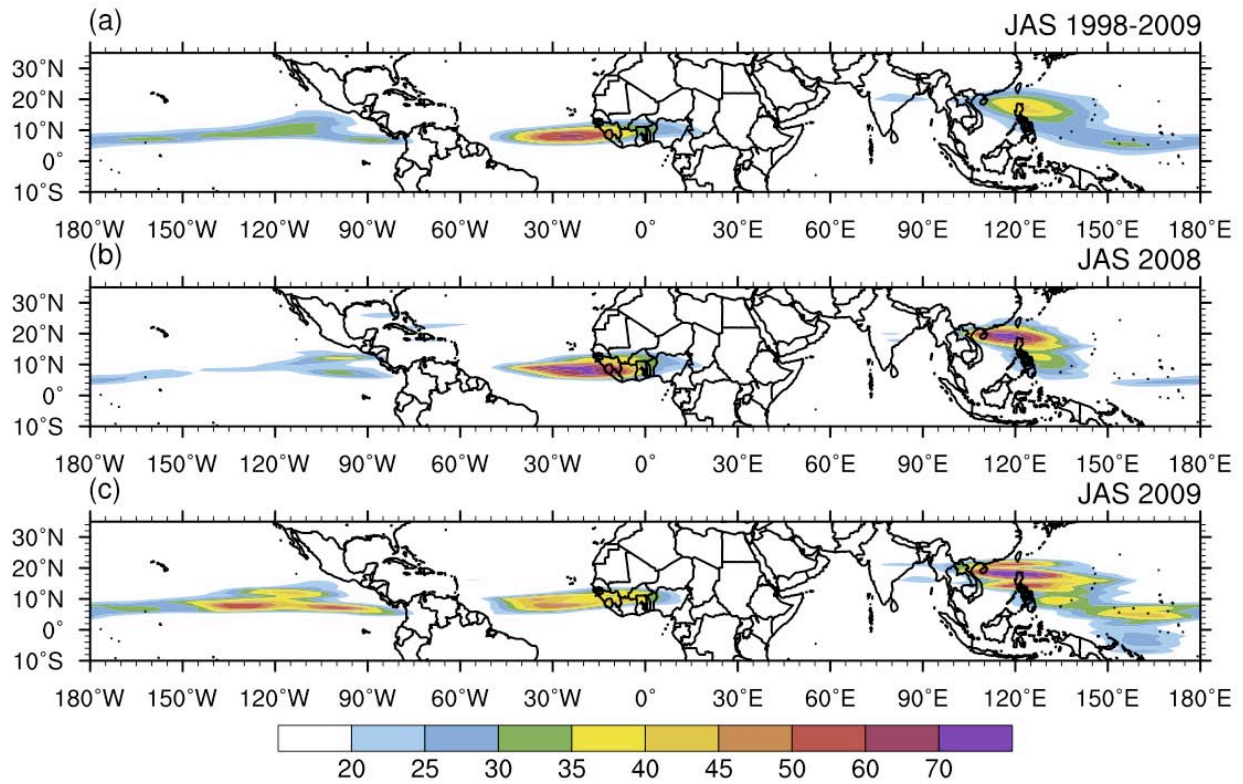
1
 2 Figure 3. Time-longitude diagram of 15°S to 15°N averaged OLR anomalies (Wm⁻²) during the YOTC period, with
 3 MJO-filtered OLR anomalies superimposed. Shading is for “total” OLR anomalies which have been temporally (7-
 4 day running mean) and spatially (R21 spectral truncation) smoothed. Contours show OLR that has been
 5 wavenumber-frequency filtered for eastward-propagating waves 1-5 and periods 30-96 days as is used to signify
 6 convective variability associated with the MJO. Contour interval is 8 Wm⁻² with dashed contours used for positive
 7 MJO-associated OLR anomalies. Labels (a)–(f) refer to the identified cases of MJO activity.



1

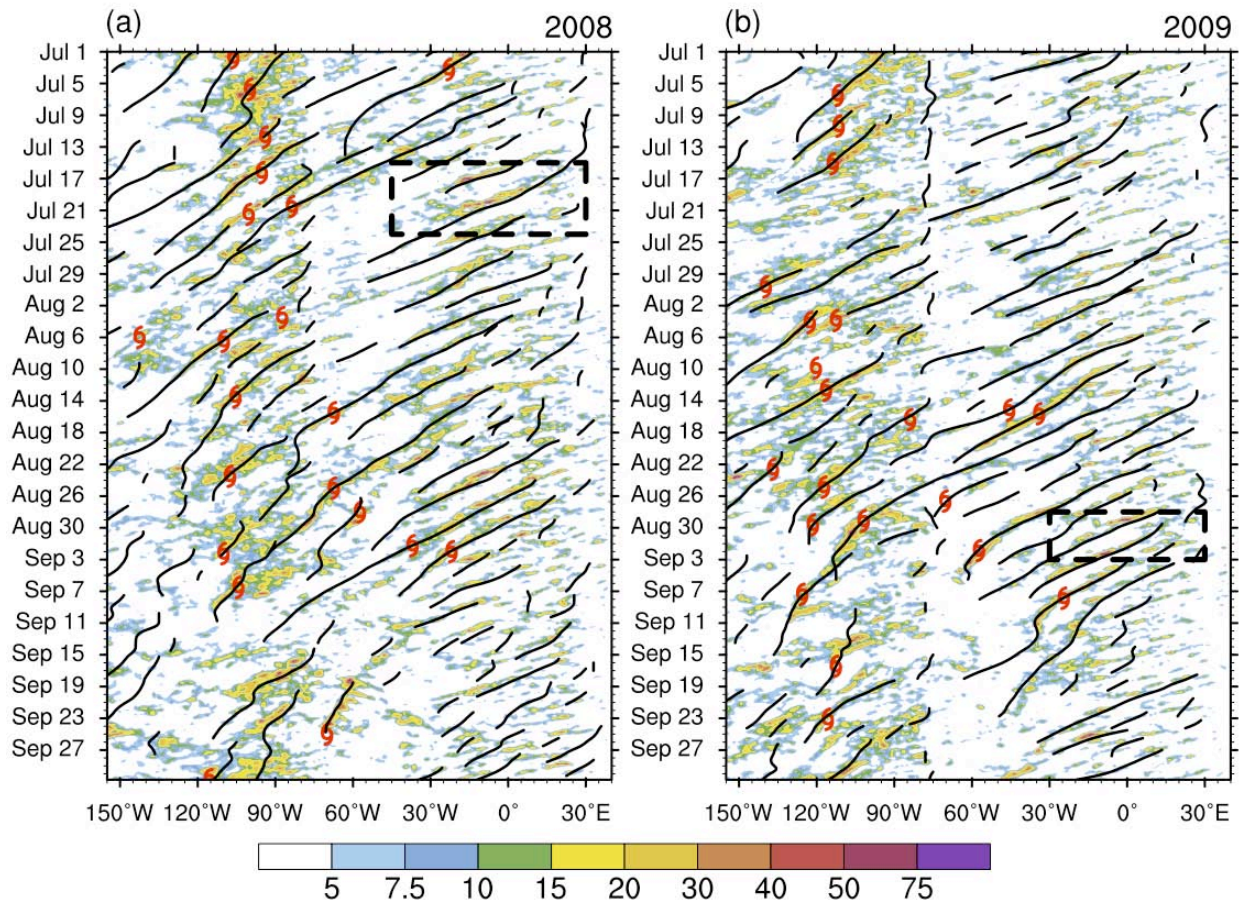
2

3 Figure 4. (top) 15°S to 15°N-averaged OLR anomalies (Wm^{-2}) for the period 20 Feb-20 May 2009, during which
 4 multiple interacting waves (MJO, equatorial Rossby, and Kelvin) existed (CCEW case #1). Shading is for the
 5 unfiltered OLR anomalies, blue contours for the MJO-filtered OLR anomalies, black contours for the n=1
 6 equatorial Rossby (ER) wave filtering, and green contours for the Kelvin wave filtering. Contour interval is 10
 7 Wm^{-2} . Postive contours for the MJO and ER wave anomalies dashed, whereas for the Kelvin wave the positive
 8 contours are omitted. (bottom) Same, except for the period 20 Feb-20 Apr 2010 (CCEW case #2).



1

2 Figure 5. Variance of TRMM3B42 TD filtered rainrate [(mm day⁻¹)²] for July-September averaged
 3 over (a) 1998-2009 (b) 2008, and (c) 2009.

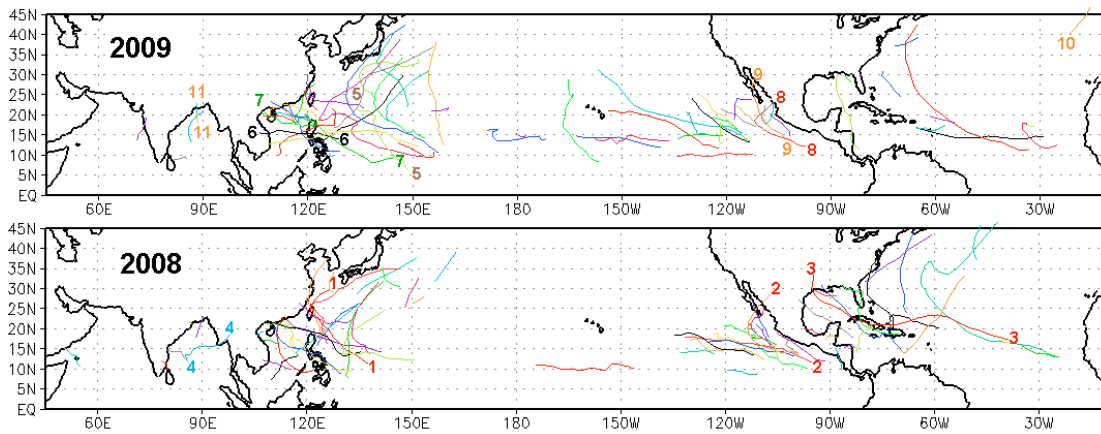


1

2 Figure 6. Hovmoller diagram of TRMM3B42 Rainrate (mm day⁻¹, shaded) averaged between 5°-20°N and
 3 objective tracks of vorticity centers exceeding 1x10⁻⁵s⁻¹ observed between 0°-30°N for (a) 2008 and (b) 2009.
 4 The time and longitude of named storm genesis is indicated by the red markers. Dashed boxes highlight periods
 5 of high impact weather referred to in the text.

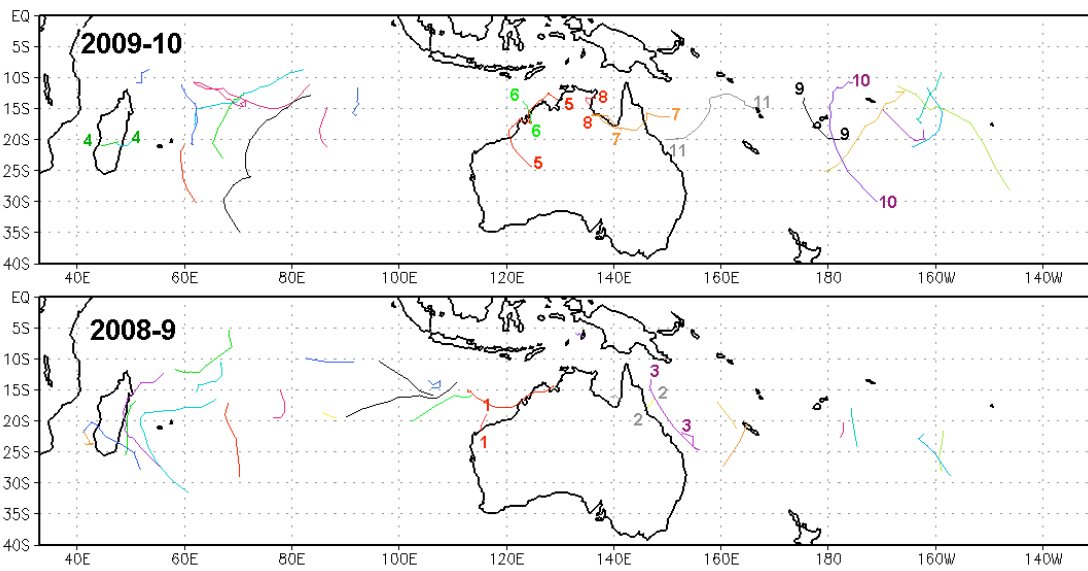
6

1 a)



2

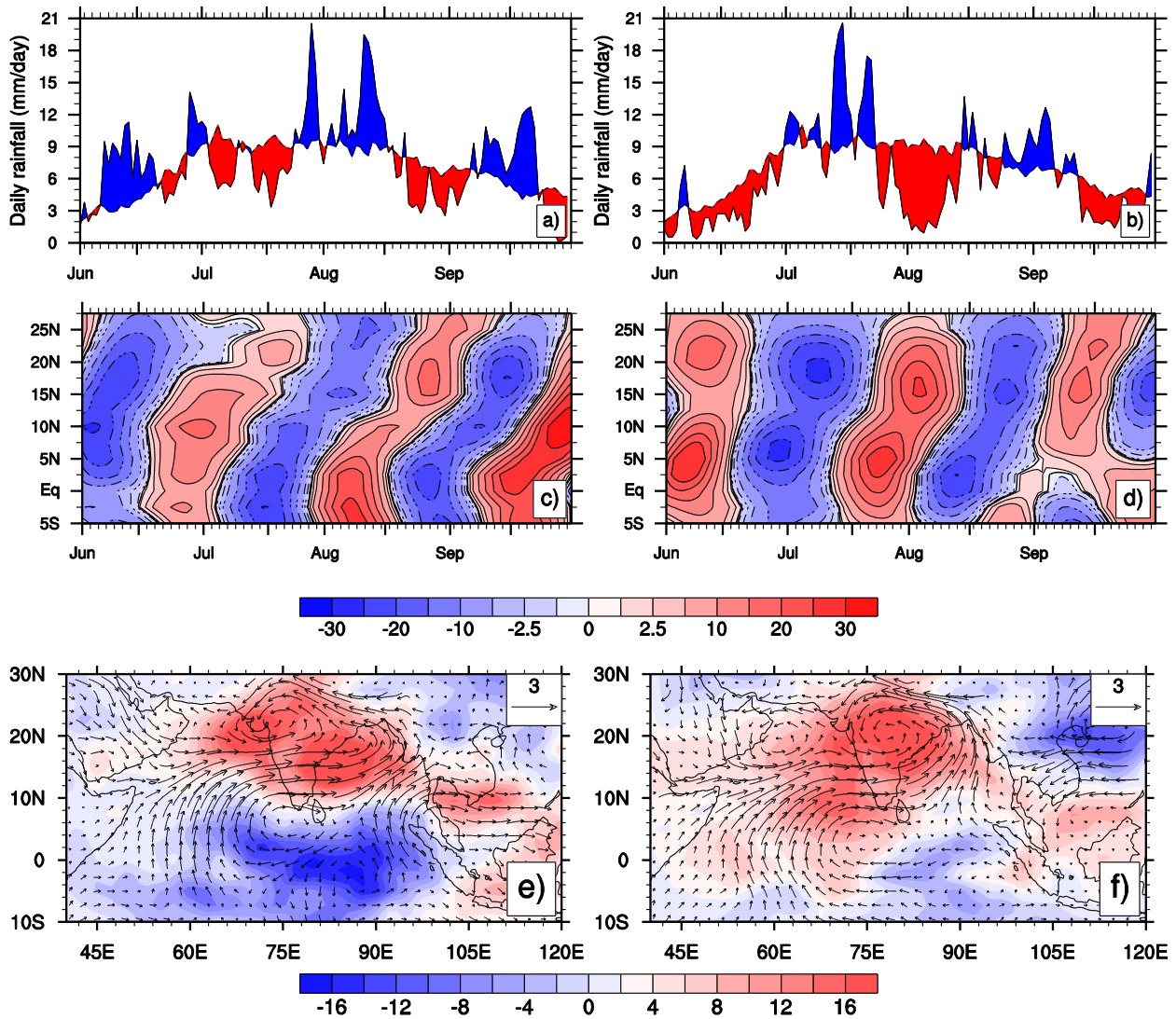
3 b)



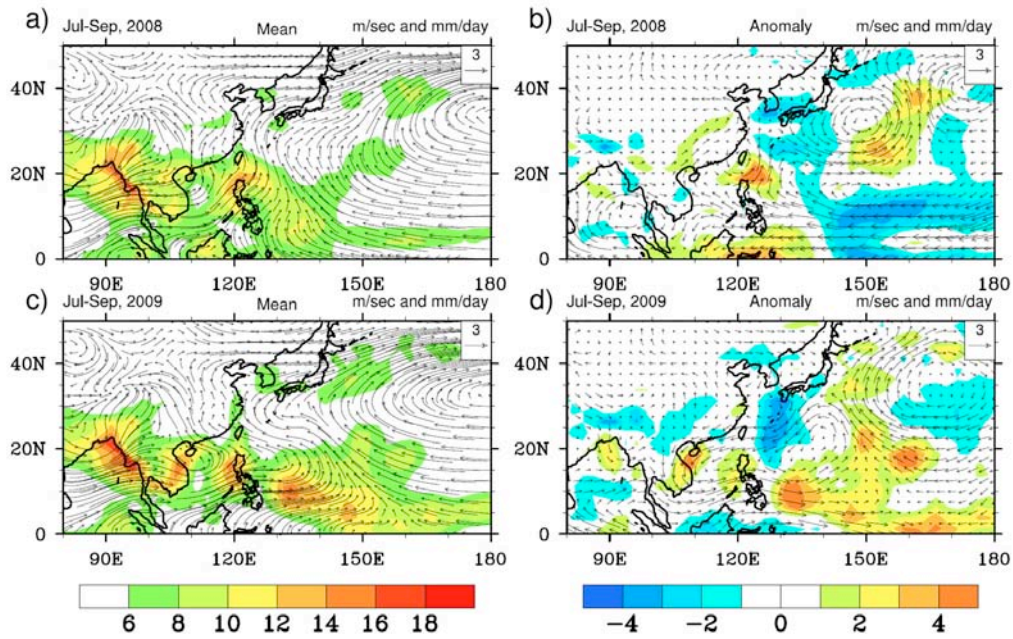
4

5 Figure 7. (a) Northern hemisphere tropical cyclone tracks. Top: 2009. Bottom: 2008. (b) Southern hemisphere
6 tropical cyclone tracks. Top: 2009-10. Bottom: 2008-9. Numbers refer to specific storms discussed in the text
7 (Section 4).

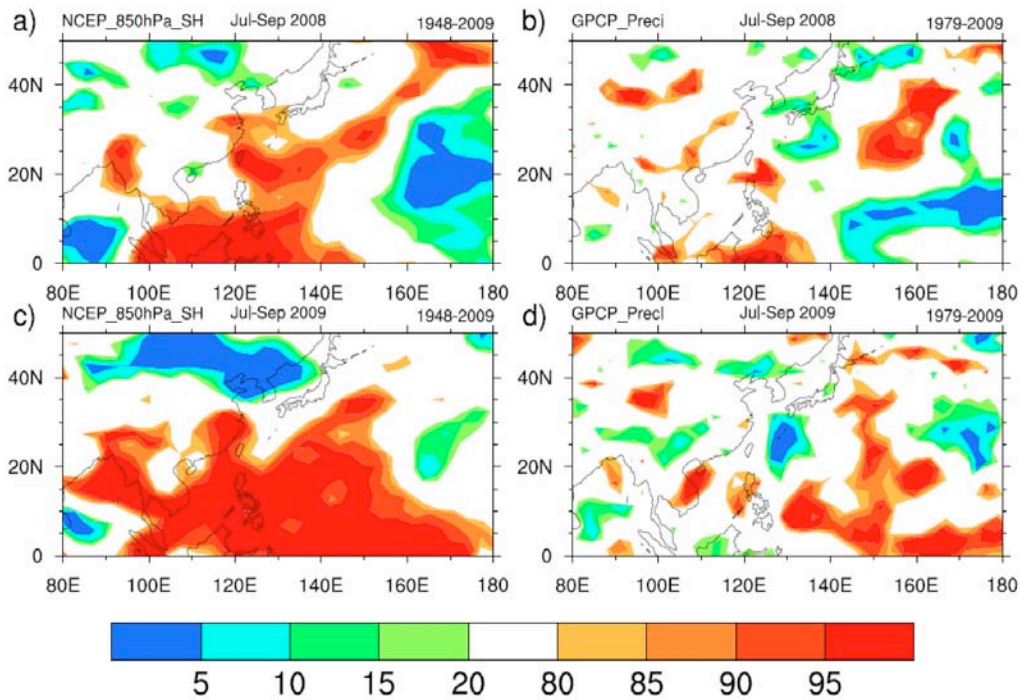
8



1
 2 Figure 8. (a) Daily rainfall (mm day⁻¹) over India (averaged between 72E-85E, 6N-27N) during 1 June-30
 3 September of 2008. Above (below) normal rainfall is shown in blue (red) on either side of the daily climatology,
 4 (b) same as (a) but for 2009. (c) Northward propagation as seen from 30-60 day filtered OLR anomalies (Wm⁻²)
 5 averaged over 60E-90E during 2008, (d) same as (c) but for 2009. (e) Lag zero regressed structure of 10-90 day
 6 filtered OLR (shaded) and 850 hPa winds with respect to a reference time series (filtered OLR anomalies
 7 averaged over central India) during 2008, (f) same as e) but for 2009.

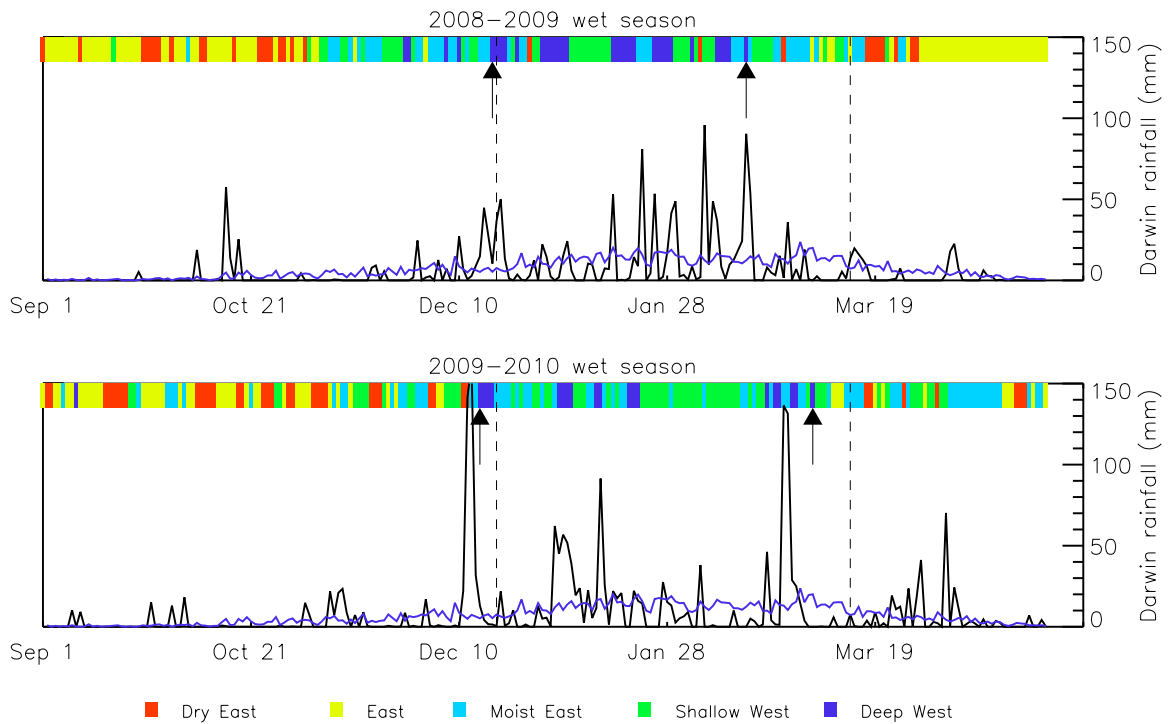


1



2

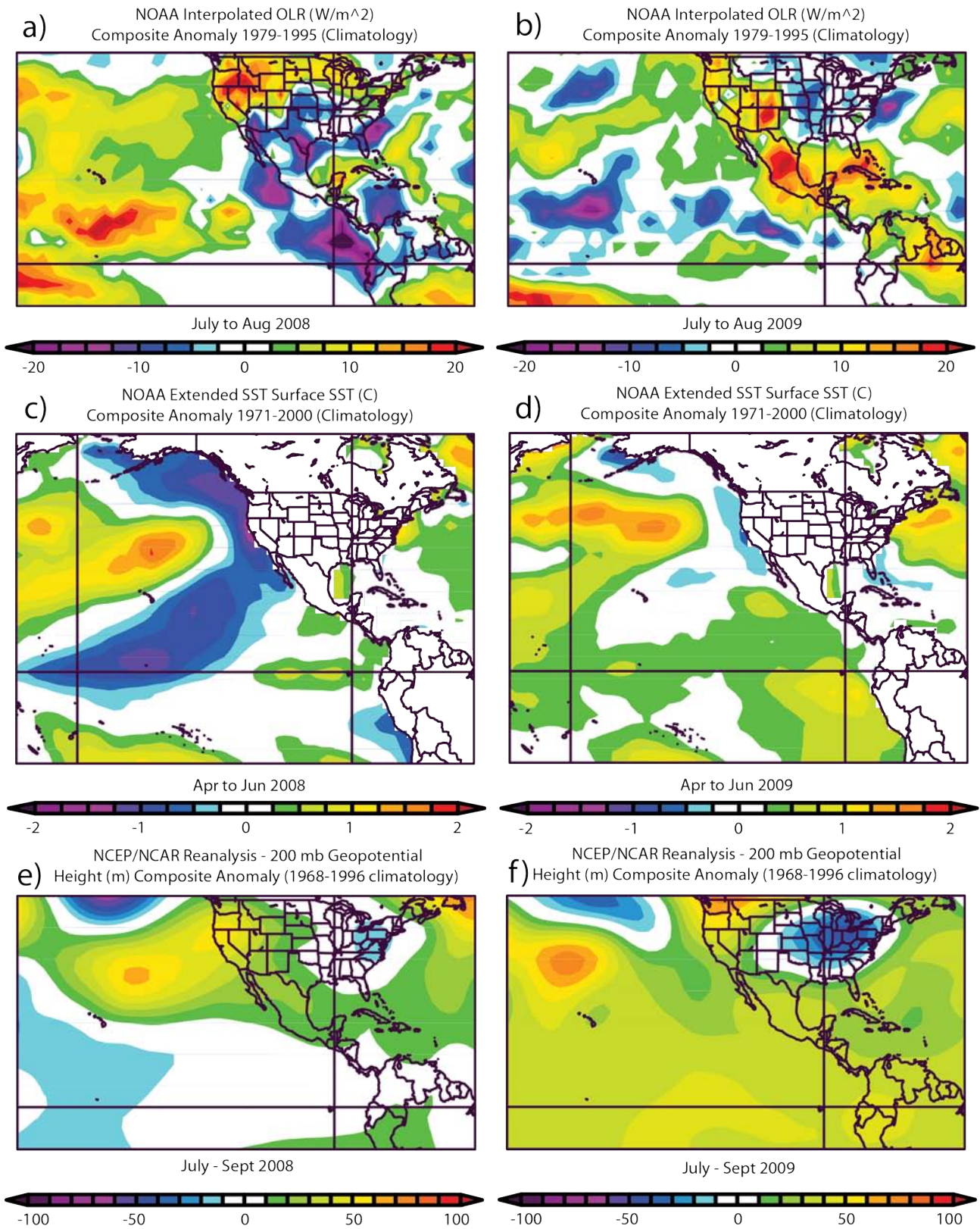
3 Figure 9. (top) Rainfall (mm day^{-1}) and 850-hPa Wind (m s^{-1}) in July-September (a) 2008 and (c) 2009. (b, d)
 4 Same as in (c, d) except for anomaly. (bottom) Distribution of percentile for (a, c) 850 hPa specific humidity and
 5 (b, d) rainfall anomalies in July-September (a, b) 2008 and (c, d) 2009. Base periods for calculating percentile are
 6 based on trying to the use as long a record as possible for the given data set selected, thus 1949-2009 and 1979-
 7 2009 for specific humidity and rainfall, respectively.



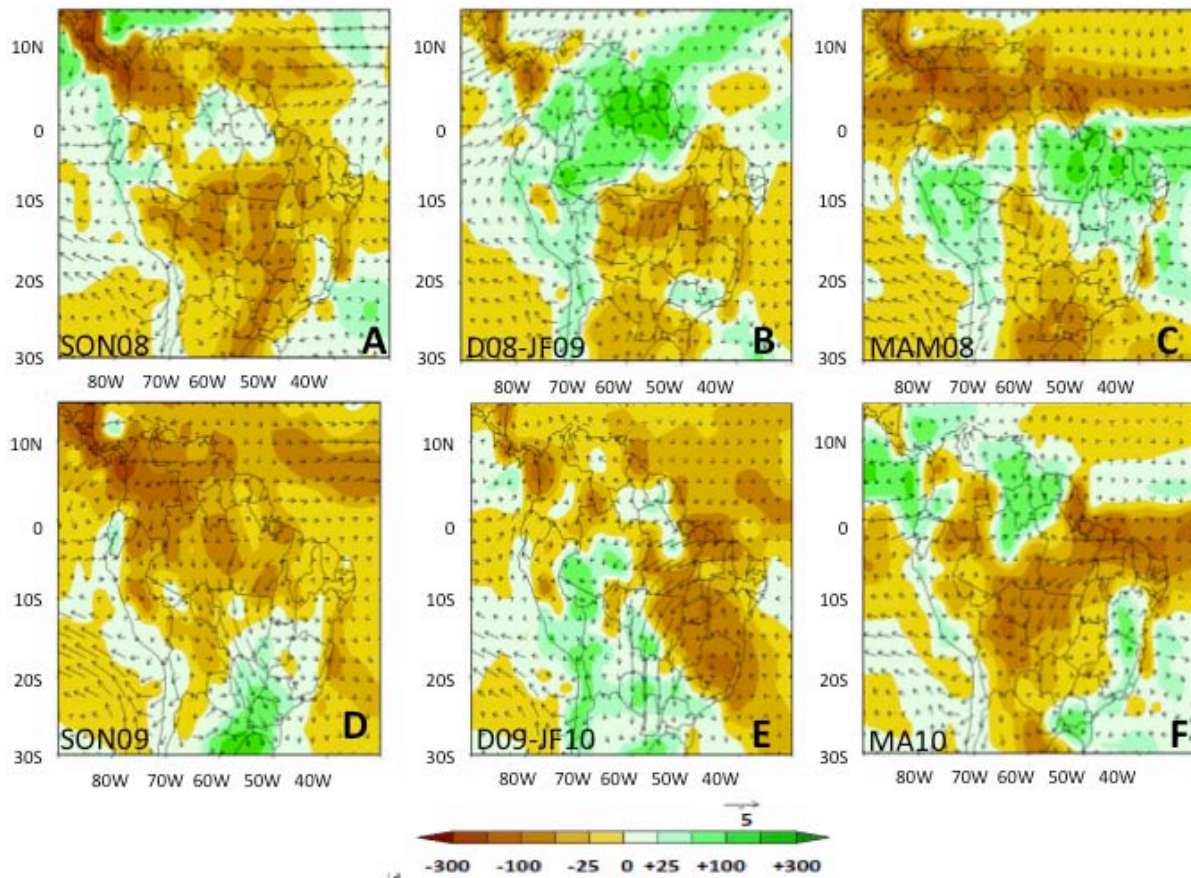
1

2 Figure 10 Time series of daily rainfall (mm; black line) and daily wet-season regime (colour bar) for the northern
 3 Australia wet seasons of 2008/09 (top) and 2009/10 (bottom). Also shown are the climatological rainfall distribution
 4 (blue line), the climatological monsoon onset and retreat days (vertical dashed lines) and the respective season's
 5 monsoon onset and retreat days (arrows) as defined in Pope et al. (2009).

6

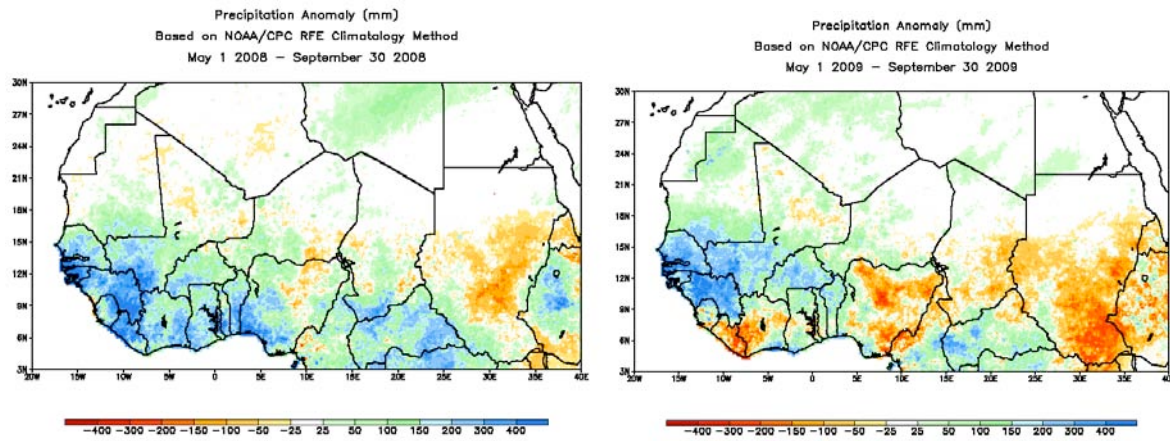


1
 2 Figure 11. Jul-Aug NOAA interpolated OLR anomalies ($W m^{-2}$; a and b), antecedent season (Apr-May-June) NOAA
 3 Extended - Optimal Interpolation (OI) sea surface temperature anomalies (C; c and d), and, Jul-Aug-Sep
 4 NCEP/NCAR reanalysis 200 hPa geopotential height anomalies (m; e and f) for 2008 and 2009, respectively.



1
2
3
4
5
6
7
8
9
10

Figure 12. Rainfall and 850 hPa winds for the South American Monsoon system. Arrow indicating wind scale (m/s) and color scale (mm) are shown in the lower side of each panel. A) September-November 2008, B) December 2008-February 2009, C) March-May 2009, D) September-November 2009, E) December 2009-February 2010 and F) March-April 2010. Sources: CPTEC/INPE. São Paulo, Brazil, and CPC-NCEP/NOAA, Maryland, US

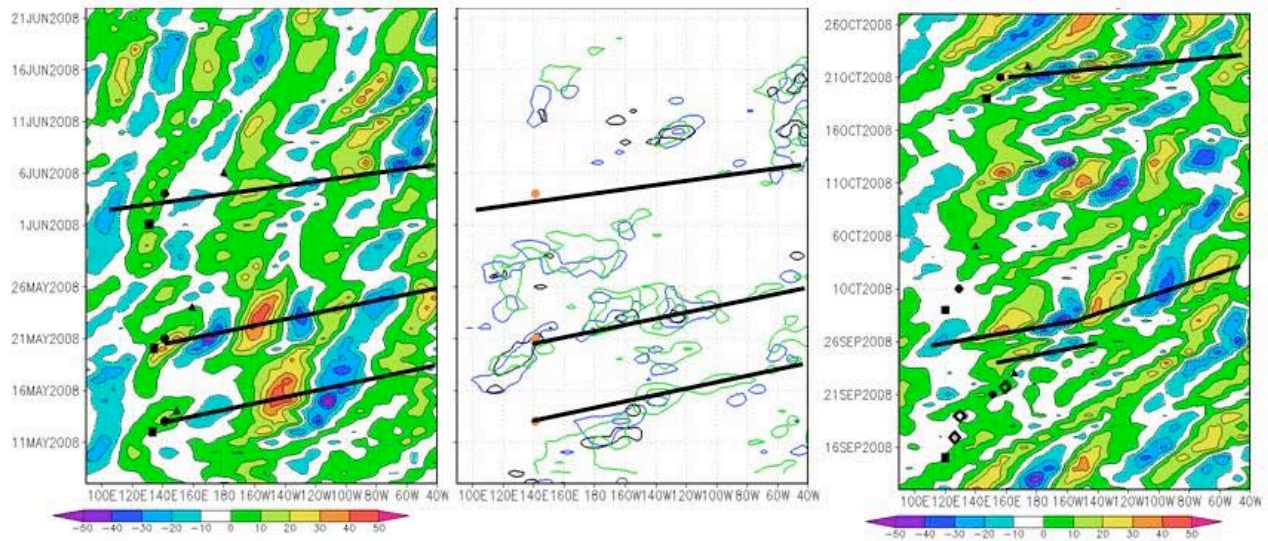


1

2 Figure 13. Seasonal precipitation anomalies (mm) for 2008 and 2009 based on May-Sep rainfall totals and with
 3 reference to a climatology based on the years 1995-2001. Precipitation is estimated using the NOAA/CPC RFE
 4 Climatology method (see http://www.cpc.noaa.gov/products/fews/AFR_CLIM/afr_clim_season.shtml for more
 5 details).

6

1

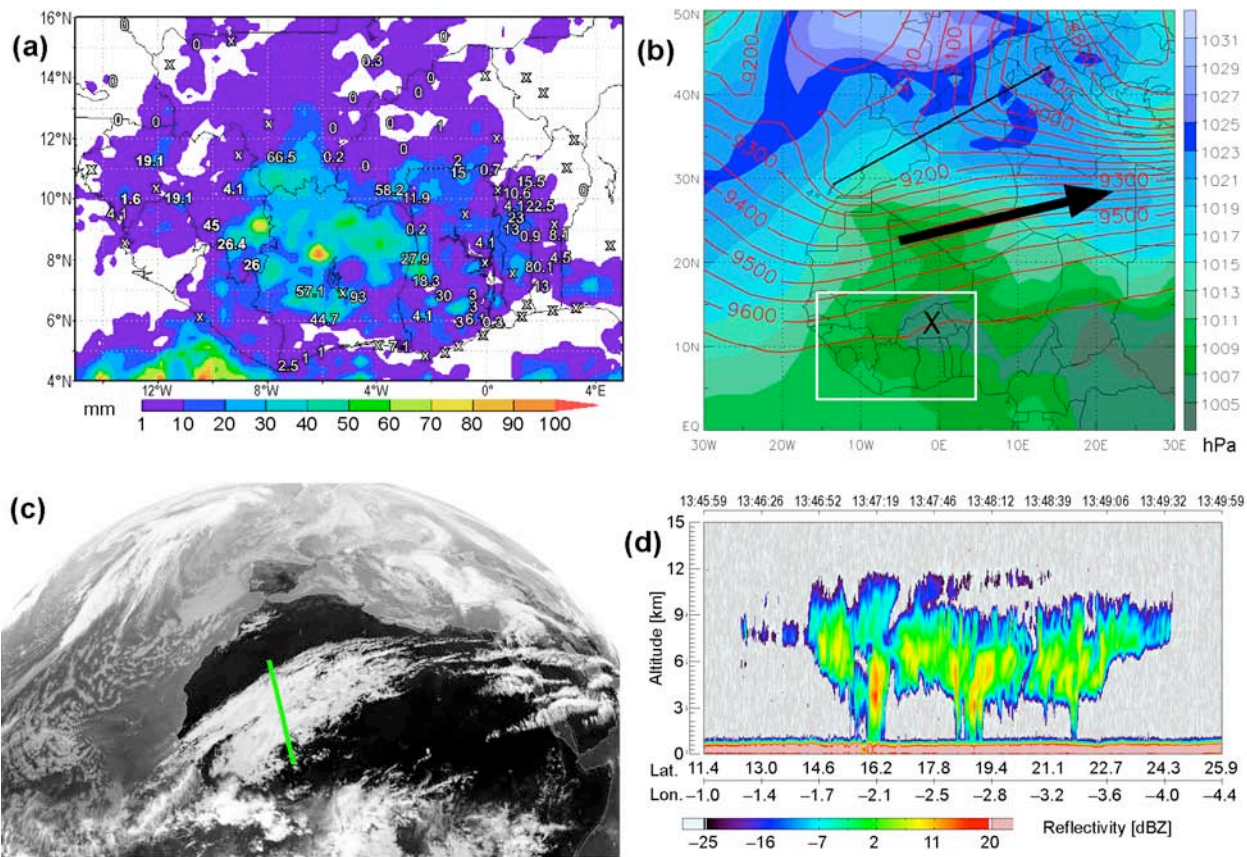


2

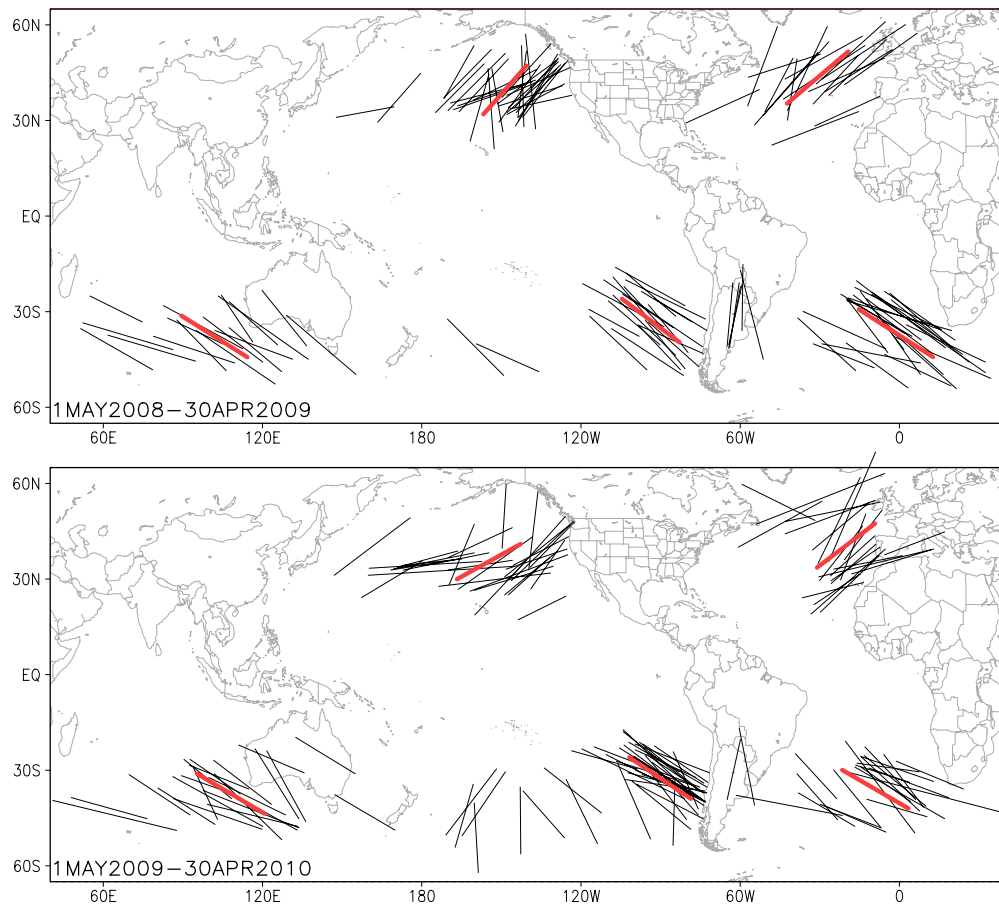
3 Figure 14. Hovmoeller plots across western North Pacific of a) 200 hPa meridional wind (m s^{-1}) from 6 May - 22
4 June 2008 averaged from 40-60 N, b) 500 hPa height standard deviation from ECMWF EPS for 3 day forecast
5 (black), 5 day forecast (blue) and 7 day forecast (green), c) as a) but from 12 September to 27 October. Typhoon
6 recurvature is marked on a) ,c) by a black square, ET by a black circle and decay point by a black triangle. The
7 red circles on b) mark the ET time. Typhoons marked are (from top to bottom) Rammasun, Halong and Nakri in
8 a),b) and Sinlaku, Jangmi and Bavi in c). Figure courtesy of Julia Keller. Data taken from the ECMWF YOTC
9 analyses and the TIGGE database.

10

1

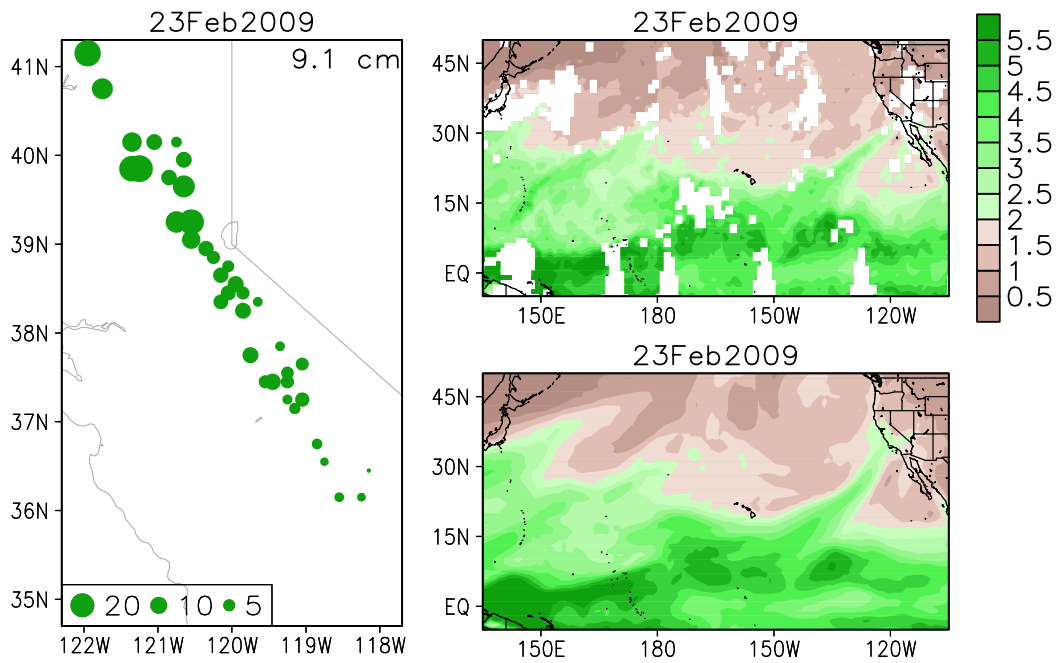


2
 3 Figure 15. An unusual dry-season rainfall event in tropical West Africa during 16–20 February 2009.
 4 (a) Precipitation accumulated over the four-day period 0600 UTC 16 Feb. to 0600 UTC 20 Feb. 2009 from the
 5 TRMM 3B42 3-hourly rainfall product (colors) and from surface rain gauges (numbers); values in mm. 'x' stands
 6 for 'no precipitation', '0' stands for 'traces of precipitation'. Some stations have gaps in their records and amounts
 7 must therefore be considered as lower bounds. (b) Geopotential height at 300 hPa (contours every 50 gpm) and
 8 mean sea-level pressure (hPa; colors) for 1200 UTC 16 Feb. 2009. Data are taken from the ECMWF YOTC
 9 analysis. The upper-trog axis, the subtropical jet streak, and the pressure minimum over Burkina Faso are
 10 indicated. The area shown in (a) is bordered by a white box. (c) Meteosat channel 9 (infrared; 10.8 μm) at
 11 1200 UTC 19 Feb. 2009. (d) Vertical profile of reflectivity (dBz) from the CloudSat Cloud Profiling Radar along
 12 the green line shown in panel (c) between 1346 and 1350 UTC 19 Feb. 2009.



1

2 Figure 16. Approximate locations (main axes; black lines) of Atmospheric Rivers (ARs) during the YOTC period.
 3 Red lines indicate the mean locations of the ARs within each ocean basin. (The few isolated ARs west of 120°W
 4 were not included in the calculation for the southeastern Pacific.) ARs are identified as long (>2000 km), narrow
 5 (<1000km) plumes of enhanced (>2 cm) integrated water vapor (IWV) in the daily maps observed by the AIRS
 6 instrument, following the criteria set in Ralph et al. (2004). The AIRS version 5 level 3 standard retrievals are
 7 used, which are globally available on a 1°×1° grid. Daily means are first formed by weighting the ascending and
 8 descending satellite passes with the number of data counts within each grid cell. (**Upper**) 1 May 2008–30 April
 9 2009. (**Lower**) 1 May 2009–30 April 2010.

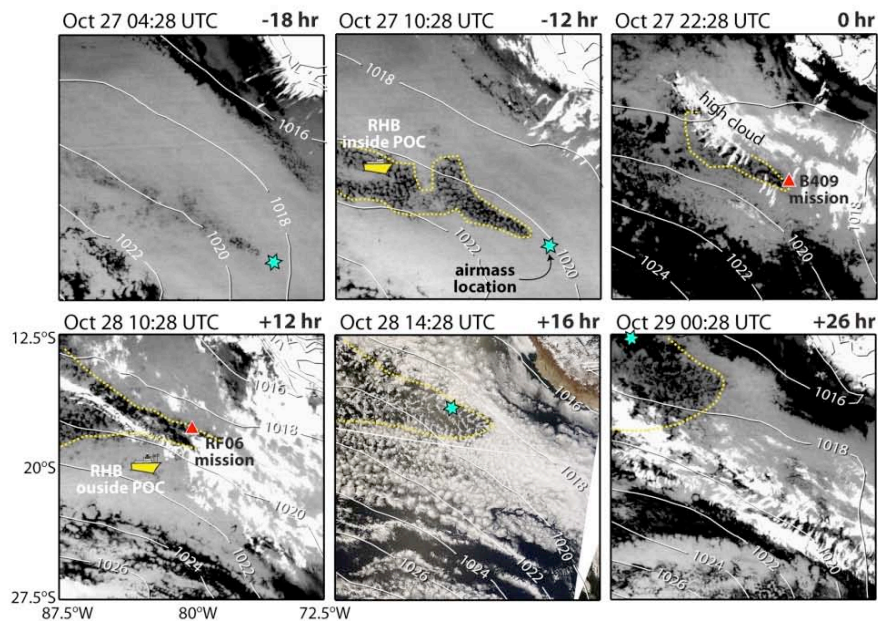


1

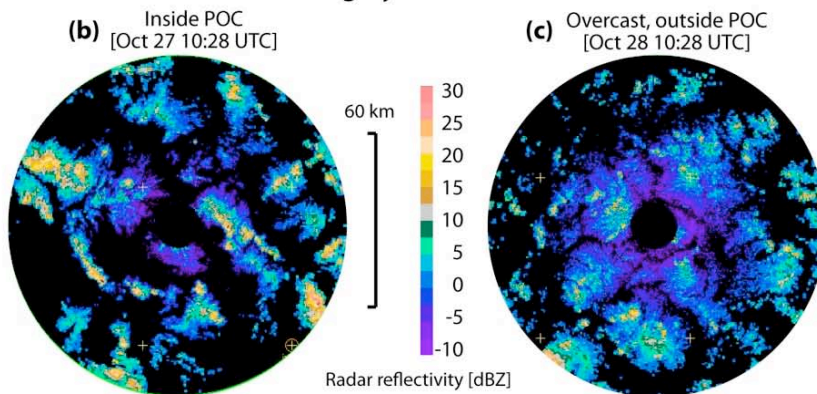
2 Figure 17. An atmospheric river (AR) event on 23 February 2009. (Left) Three-day cumulative precipitation (cm;
 3 centered on the AR date) observed at snow sensor sites across the Sierra Nevada. Data were obtained from the
 4 California Department of Water Resources (<http://cdec.water.ca.gov/>). Domain averaged precipitation is
 5 indicated in the upper right corner of the panel. (Right) Daily mean integrated water vapor (cm; IWV) from
 6 (upper right) the AIRS instrument and (lower right) the ECMWF YOTC data set.

7

(a) Geostationary satellite imagery



C-band radar imagery from the Ronald H Brown



1

2 Figure SIDEBAR 1: (a) Thermal infrared and visible (Oct 28 14:28 UTC only) imagery for a 44 hour period
3 encompassing the intensive measurement period in which a pocket of open cells (POC) is sampled by two
4 aircraft (FAAM BAe-146 mission B409 and NSF/NCAR C-130 mission RF06) and the NOAA R/V Ronald H. Brown
5 (RHB). The POC is delineated by the dashed yellow line. The blue star shows the location along a 925 hPa
6 trajectory of an air parcel initiated at the location/time shown in the upper left panel. These locations are
7 indicated by red triangles for the images when the aircraft were sampling. (b,c) Images of radar reflectivity from
8 the C-band radar on the RHB for periods when the ship was inside the POC (b, see upper central satellite image
9 for ship location) and outside the POC (c, see lower left satellite image for location of ship).

10

11